Supermassive black hole mergers and their gravitational radiation

László Árpád GERGELY

University of Szeged, Hungary

2012

Introduction: black holes

Prediction 1) Light is curved by mass / energy (general relativity)

Our Sun:

- deflection of light calculated as

$$\Delta\phi = \frac{4GM}{c^2 b}.$$

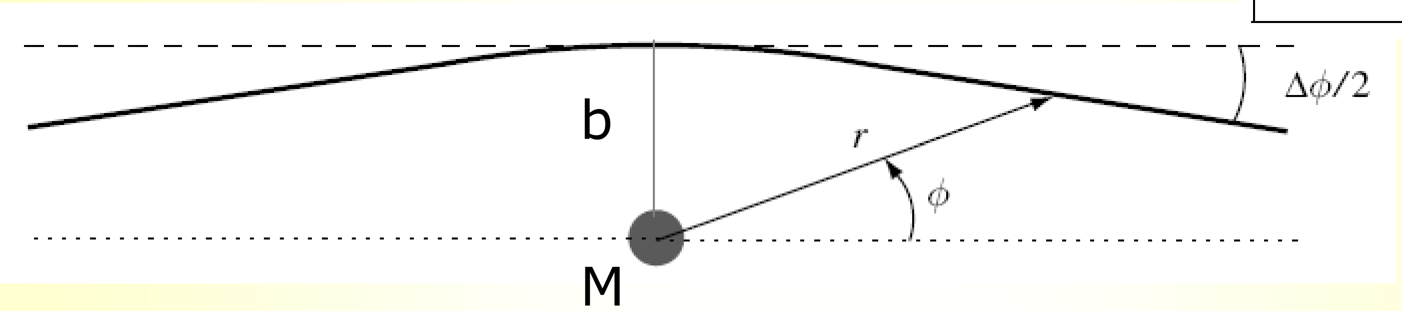

- numerically for the light ray passing near the Sun $\Delta\phi = 1''.75$

- Eddington 1919:

$$\Delta\phi = 1''.98 \pm 0''.16,$$
$$\Delta\phi = 1''.61 \pm 0''.4,$$

→ Einstein got famous

What is a black hole, again?

Prediction 2)* *Gravity is attractive (→ some of us work in the field ☺), ***and increases with the mass***

→ ***After the nuclear "fuel" is consumed, no mechanism (not even quantum) to balance the gravitational collapse of a star > few solar masses (see next slide)***

→ ***Light can get extremely curved***

→ ***Regions of space where the light cannot escape from!!!***

they look black;

things can fall in, not out (gravity attractive)

→ ***Black holes***

When is a black hole formed?

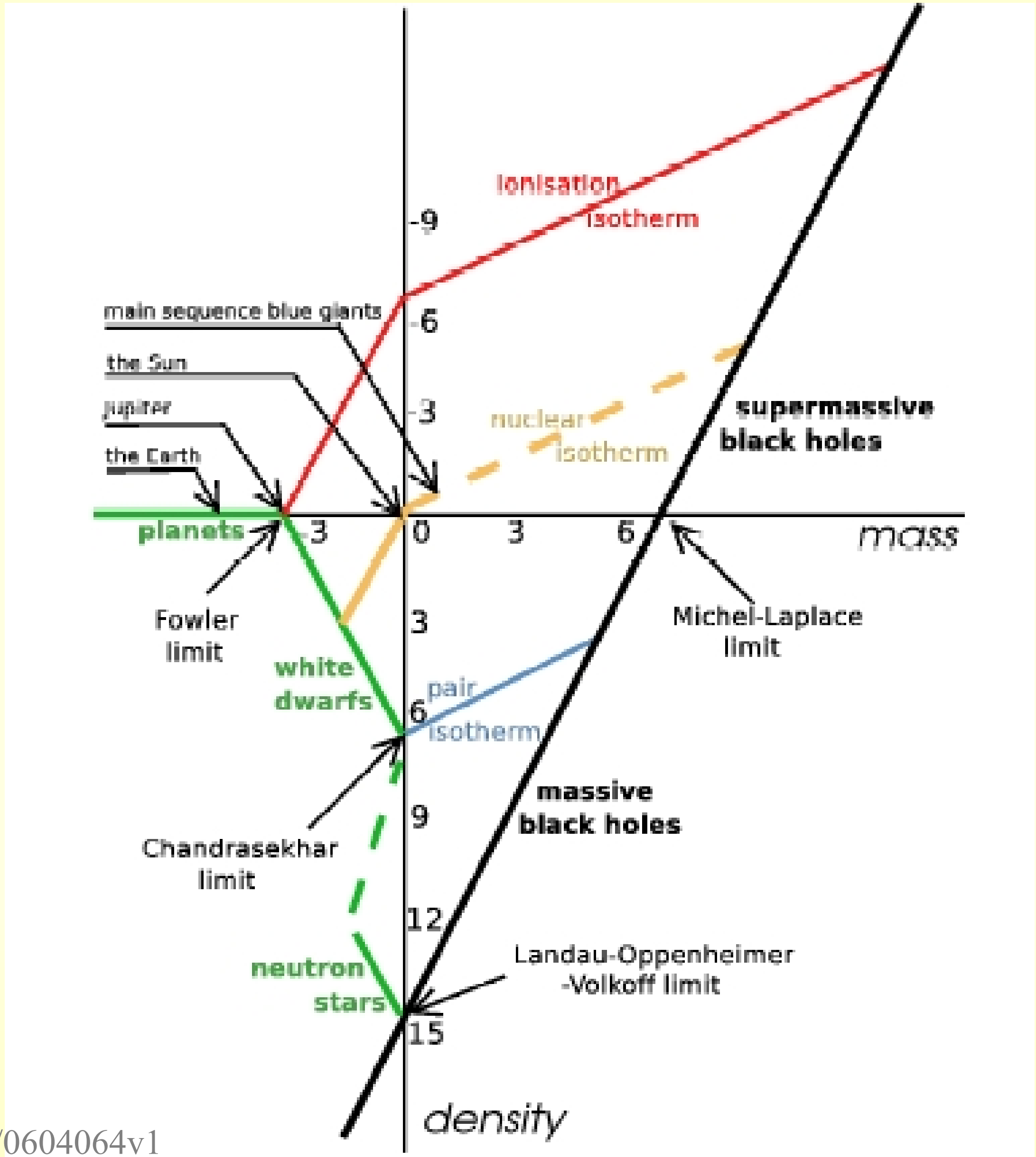

B. Carter: arXiv:gr-qc/0604064v1

Space-time representation / diagram

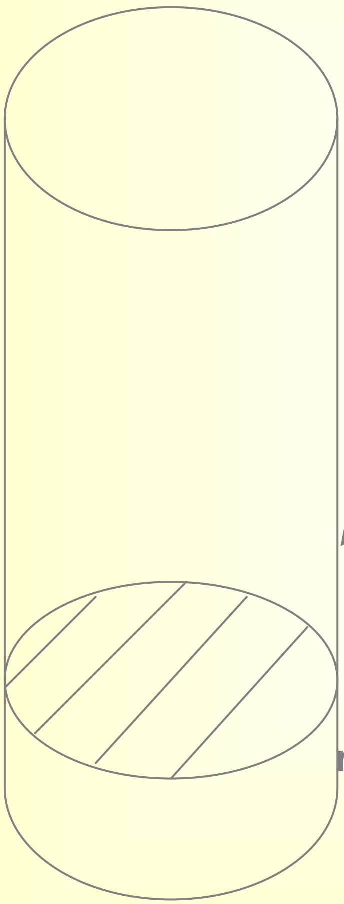

time

horizon

Instead of 3 spatial dimensions we can represent but 2;

then the circle represents a sphere instead

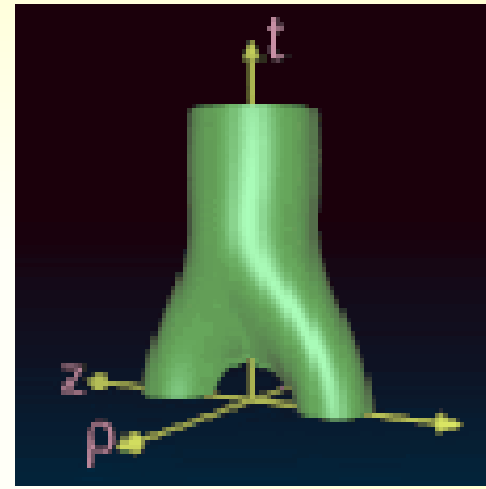

Space-time representation of merging BHs

Schwarzschild black hole (1916)

- vacuum condition $R_{ab} = 0$
- spherically symmetric, static, asymptotically flat

$$ds^2 = -f(r)dt^2 + f^{-1}(r)dr^2 + r^2 d\Omega^2 \,,$$

$$f(r) = 1 - \frac{2Gm}{c^2 r} \,.$$

- m central mass, t Killing time, r curvature coordinate
- $r=0$ curvature singularity $R^{abcd}R_{abcd} \propto m^2 r^{-6}$
- $r=2Gm/c^2$ event horizon / only coordinate singularity / (not even radial outward directed light can escape)

Gravitational collapse leading to Schwarzschild BH

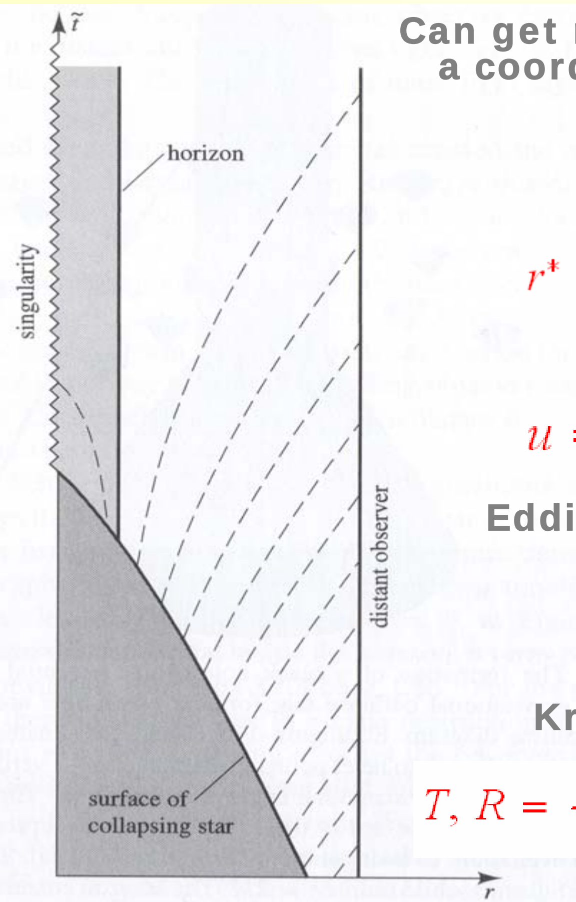

Can get rid of the coordinate-singularity by a coordinate transformation (singular itself on the horizon).

Tortoise coordinate:

$$r^* = r + \frac{2Gm}{c^2} \ln \left| 1 - \frac{c^2 r}{2Gm} \right|$$

Null coordinates:

$$u = t - r^* , \qquad v = t + r^*$$

Eddington-Finkelstein coordinates:

either (u, r) or (v, r)

Kruskal-Szekeres coordinates:

$$T, R = \frac{1}{2}\left[\exp\left(\frac{c^2 v}{4Gm}\right) \mp \exp\left(-\frac{c^2 u}{4Gm}\right) \right]$$

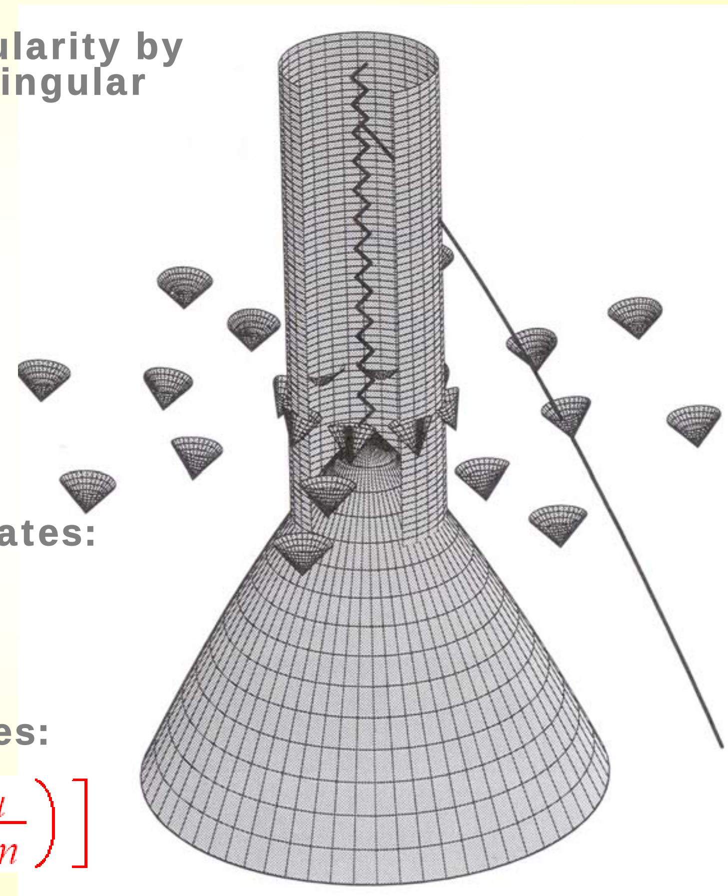

Hartle: *Gravity*2003

Eternal Schwarzschild BH

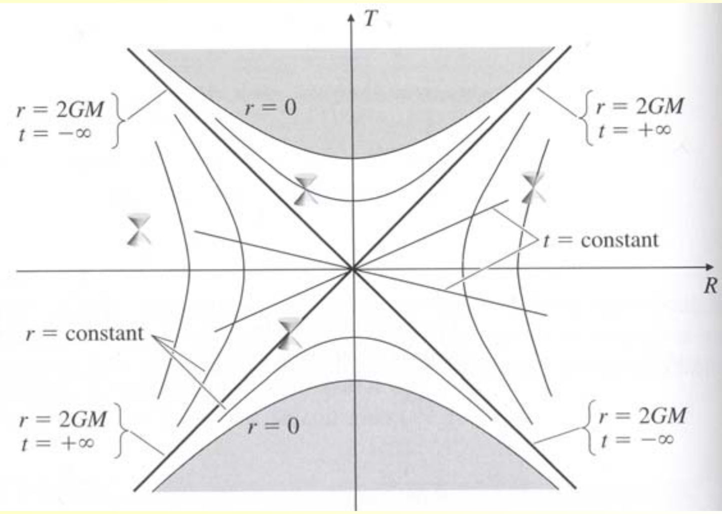

Carroll: *Spacetime and Geometry* 2004

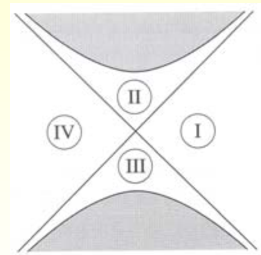

I. Outer region (right static region)

II. Extension below the horizon (future dynamic region)

III. Past dynamic region (white hole; II. time-reflected)

IV. Left static region (a second copy???)

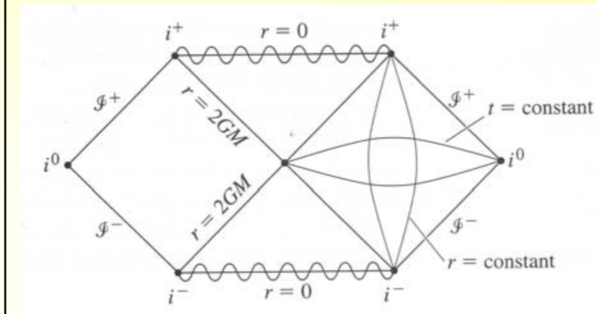

FIGURE 5.16 Conformal diagram for Schwarzschild spacetime.

Penrose-Carter diagram

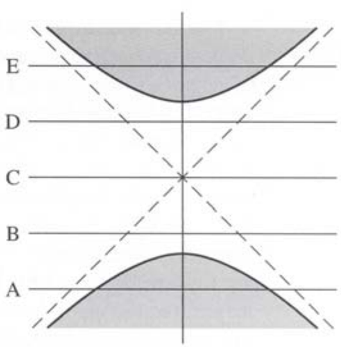

FIGURE 5.14 Spacelike slices in Kruskal coordinates

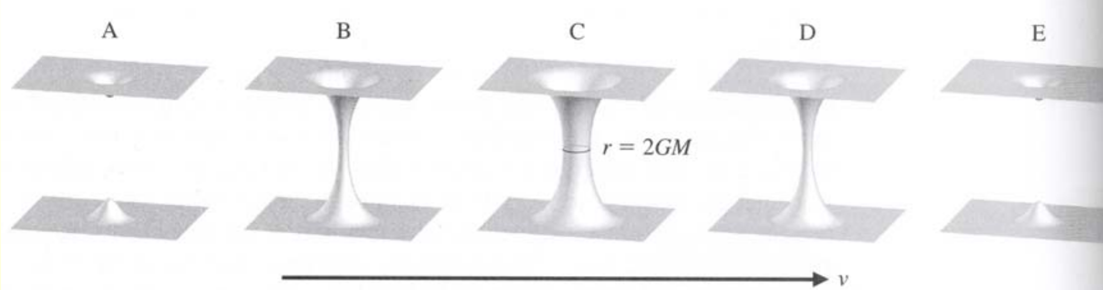

FIGURE 5.15 Geometry of the spacelike slices in Figure 5.14.

wormhole / Einstein-Rosen bridge

The taxpayer and Professor Visser….

Dear Professor,

I am deeply disturbed, I red your book and think I have a wormhole in my head. [...]

Signed: *******

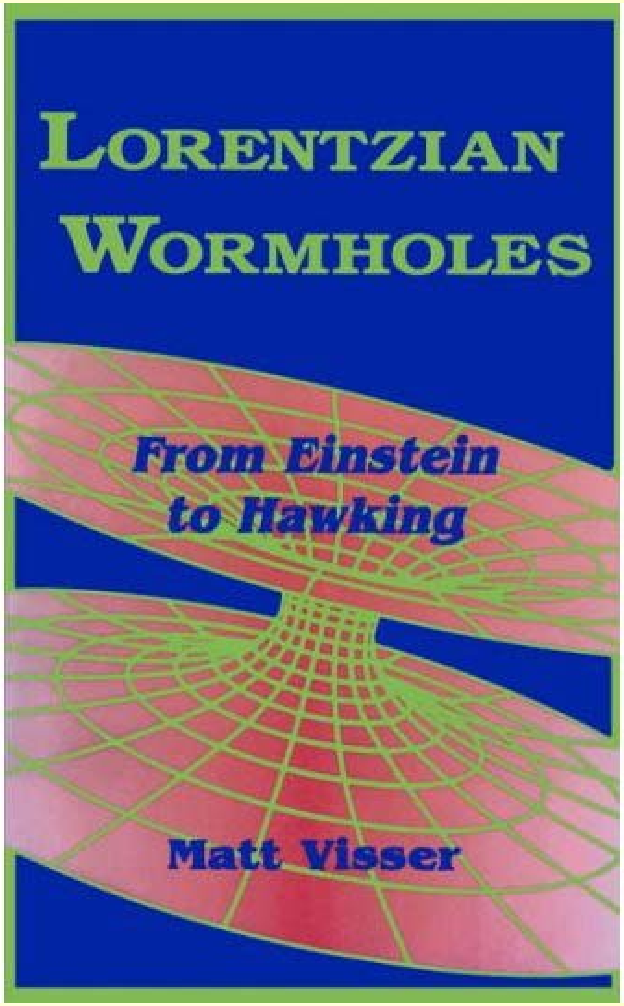

Other famous BHs

Reissner-Nordström spherically symmetric ***electro-vacuum***:

$$ds^2 = -f(t,r)dt^2 + g^{-1}(t,r)dr^2 + r^2 d\Omega^2 \,,$$

$$f(r) = g(r) = 1 - \frac{2Gm}{c^2 r} + \frac{G\left(Q^2 + P^2\right)}{r^2}$$

Q electric charge

P magnetic charge

Vaidya-(Anti) de Sitter spherically symmetric ***radiation field*** in geometrical optical limit (null dust) + ***cosmological constant*** Λ

$$f(v,r) = g(v,r) = 1 - \frac{2Gm(v)}{c^2 r} - \frac{\Lambda}{3} r^2$$

Kerr-Newman stationary, axially symmetric, asymptotically flat, convex event horizon

Vacuum: 2 parameters: ***mass*** + ***rotation*** parameter → Kerr

Electro-vacuum: additional ***charge*** parameter → Kerr-Newman

Famous theorems / conjectures on BHs

Unicity theorems for vacuum: Robinson (Kerr); Israel (Schwarzschild)

Singularity ***theorems***: Penrose, Hawking (the singularity at the center of the BH is ***not due to the highly symmetric setup***)

Cosmic censorship conjecture: each singularity remains hidden below a horizon (when asymptotic flatness & dominant energy condition obeyed)

BHs in the laboratory?

Analogue BHs Acoustic (dumb and deaf) holes in Bose-Einstein condensates: the sound is trapped below a supersonically flowing surface

Optical BHs “slow light” small (even zero) group velocity of light

Condensed matter analogues quantum tunnelling in some sense analogue to Hawking radiation

What is the Hawking radiation of BHs?

When vacuum fluctuations create a virtual particle pair in the vicinity of the EH, the one with negative mass falls more likely below the horizon

→ *the positive mass virtual particle emerges into the real world*

→ *this stream of particles leaving the BH appears as the BH was radiating = Hawking radiation*

(this is a semi-classical effect !)

Predictions: 1. radiation levels from large (thermodynamically cold) BHs are very low → *astrophysical detection of HR impossible*

2. small (thermodynamically hot) BHs evaporate fast → *no dangerous BHs from LHC*

Open issues in BH research

- definition of the BH horizon in non-stationary cases
- unicity theorems mostly unproved in higher dimensions (stringy BHs) and for alternative gravity BHs
- interpretation issues in BH geometro-thermodynamics
- BH perturbations not always well understood
- no known interior for Kerr
- BH environment (accretion, jet phenomenology) needs better understanding
- the science of gravito-magneto-hydrodynamics
- BH quantization

Supermassive black holes

The SMBH in the center of the Milky Way

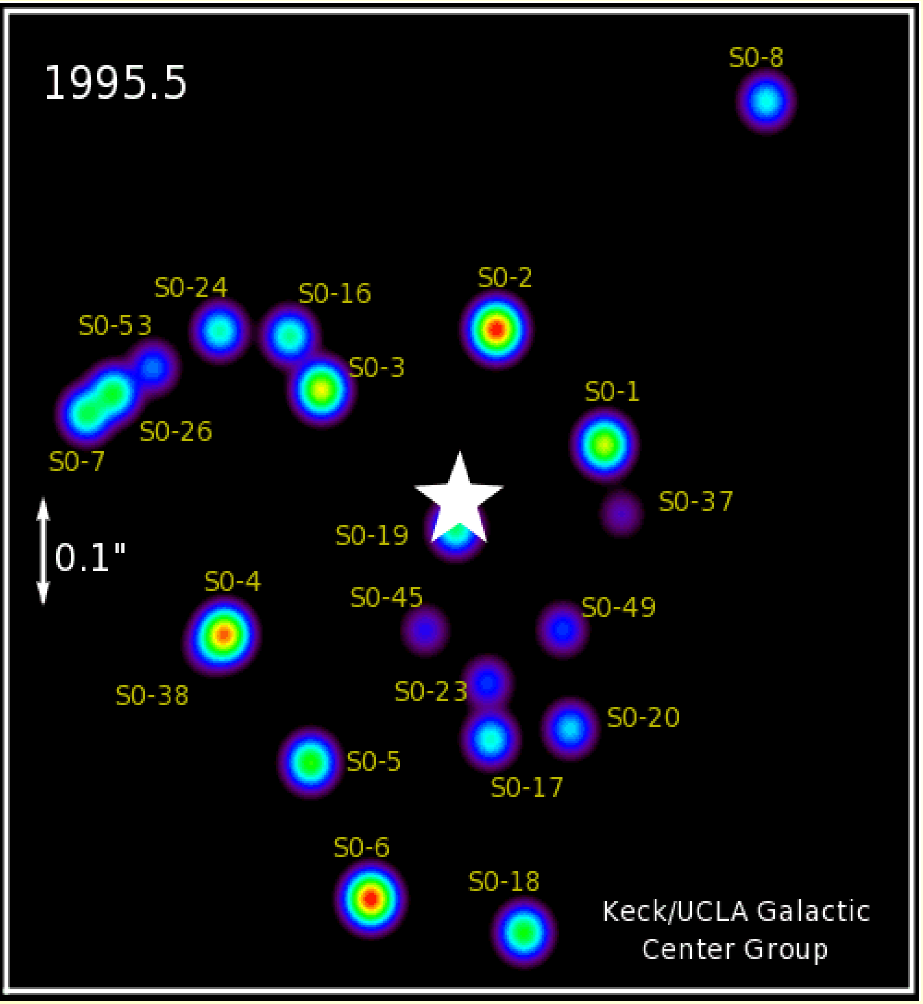

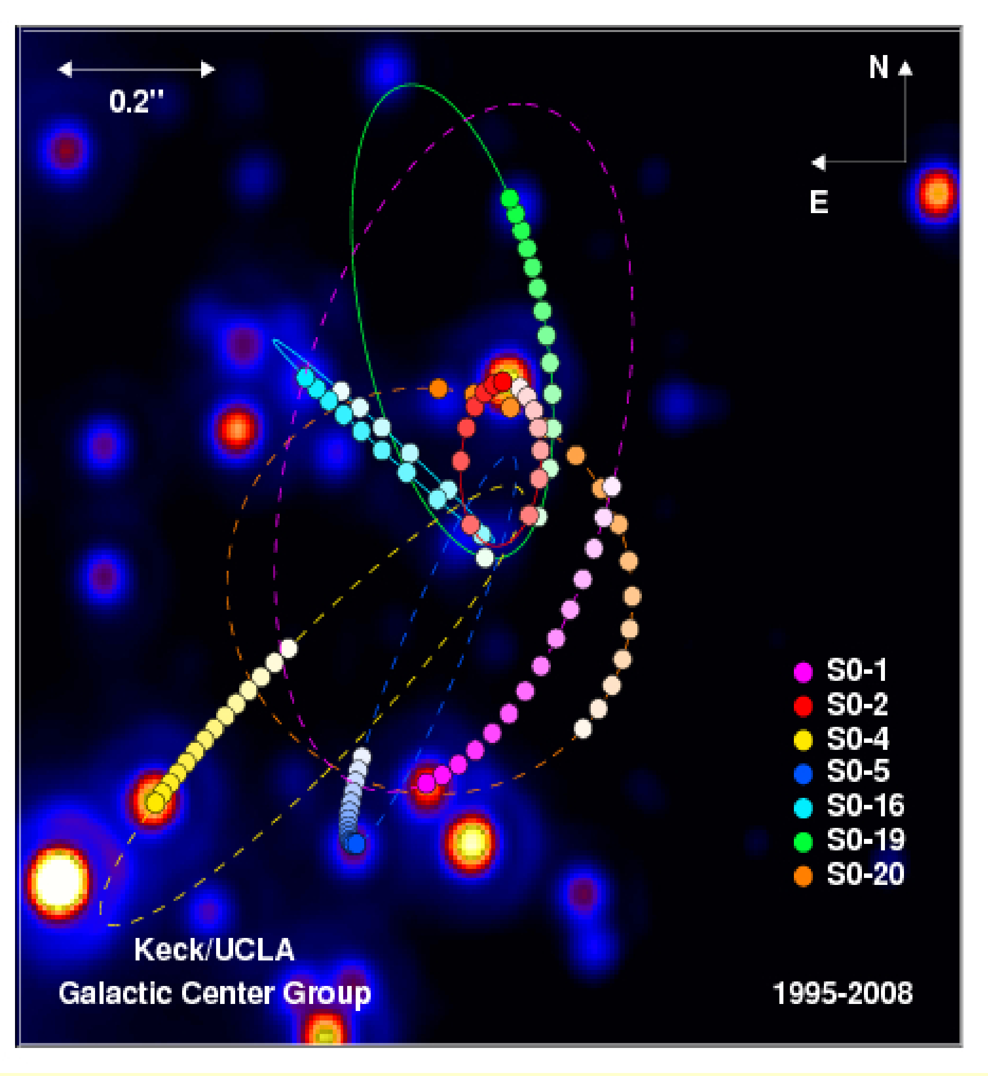

The sky in SMBHs

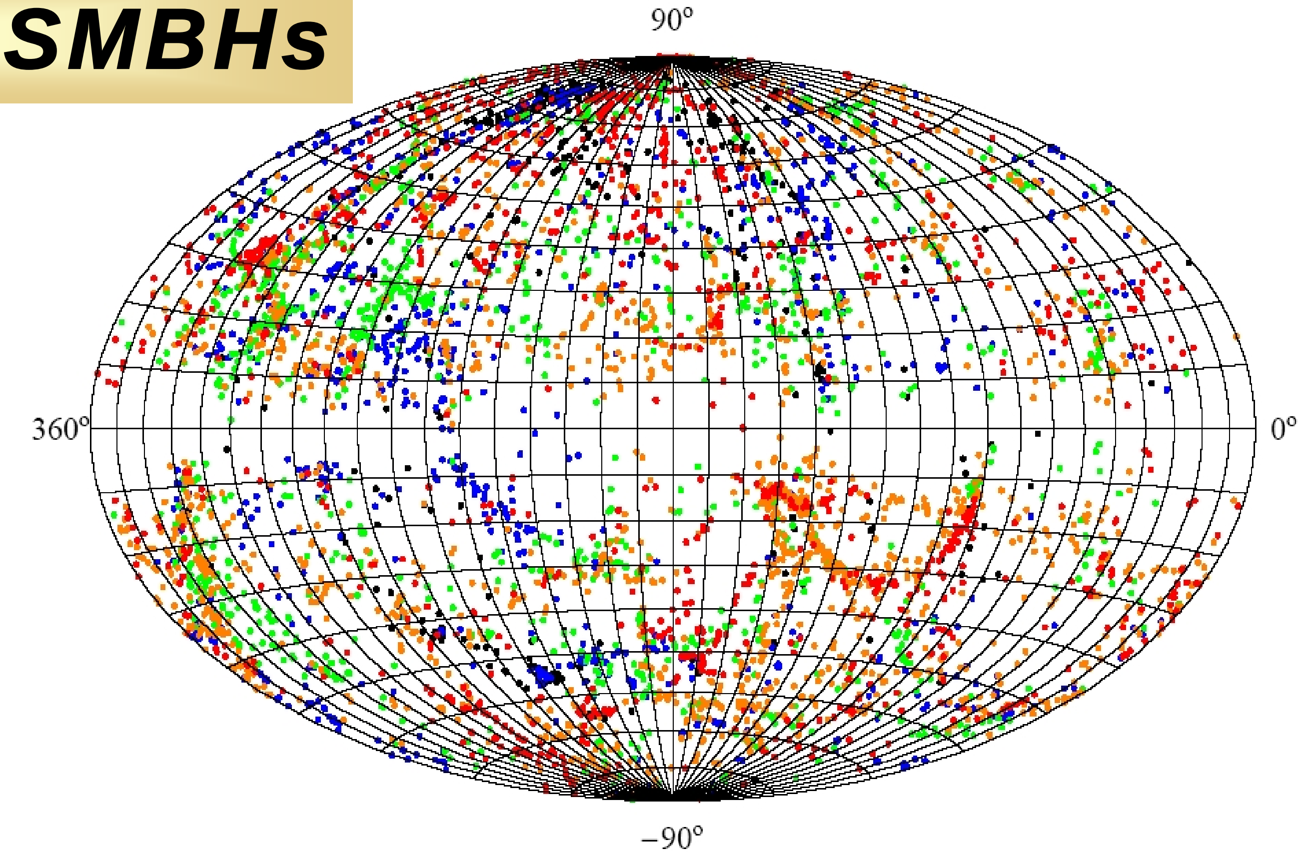

Figure 5 The sky in black holes, $\gtrsim 10^7\ M_\odot$: Aitoff projection in galactic coordinates of 5,978 candidate sources in the case of a complete sub sample (the Galactic plane remains obscured). The choice was made from a complete sample of 10,284 candidate brighter than 0.03 Jy at 2 micron, and selected at z< 0.025; this uses the 2 micron all sky survey, limited in a 20 degree band in the Galactic plane. These candidate sources are probably all black holes, with masses near to or above 10^7 solar masses; the black hole mass was determined with the black hole versus mass spheroidal stellar population correlation, and tested. The color code is Black, Blue, Green, Orange, Red corresponding to redshifts betwen 0, 0.005, 0.01, 0.015, 0.02, 0.025: Caramete et al. 2008

The sky in SMBHs II.

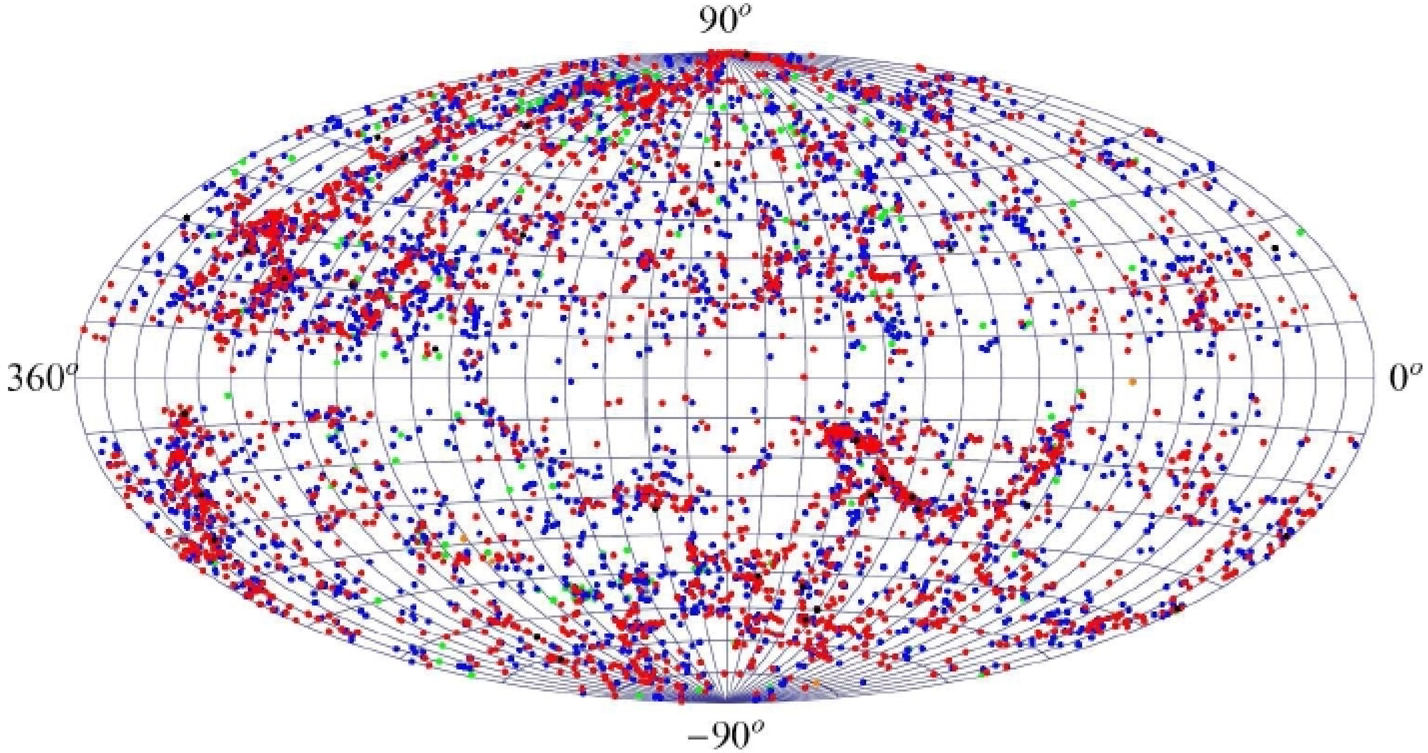

Figure 1. Aitoff projection in galactic coordinates of 5,895 NED SMBH candidate sources. The complete sample is complete in a sensitivity sense, in order to derive densities one needs a volume correction. The color code is Orange, Green, Blue, Red, Black corresponding to masses above $10^5 M_\odot$, $10^6 M_\odot$, $10^7 M_\odot$, $10^8 M_\odot$, $10^9 M_\odot$, respectively. With the exception of the less numerous first range (Orange), representing compact star clusters, the rest are SMBHs.

L. Á. Gergely, P. L. Biermann, L. I. Caramete: *Class. Quantum Grav.* 27 194009 (2010)

SMBH mass function

The mass distribution $\Phi_{BH}(m)$ of the galactic central SMBHs in the mass range $10^6 \div 3\times10^9$ solar masses ($M_\odot$) well described by a broken powerlaw

[1] W. H. Press, P. Schechter, *Astrophys. J.* **187**, 425 (1974)
[2] A. S. Wilson, E. J. M. Colbert, *Astrophys. J.* **438**, 62 (1995)
[3] T. R. Lauer et al., *Astrophys. J.* **662**, 808L (2007)

Confirmed by observational surveys

[4] L. Ferrarese et al., *Astrophys. J. Suppl.* **164**, 334 (2006)
[5] L. I. Caramete, P. L. Biermann, *Astron. Astroph.* **521**, A55 (2010)

Break at about $10^8 M_\odot$,
$\Phi_{BH}(m)\sim m^{-1}$ below and
$\Phi_{BH}(m)\sim m^{-3}$ above.
The fit with [5] gives

$$m_* = 10^{7.95}\mathrm{M}_\odot \approx 8.9\times10^7\mathrm{M}_\odot$$

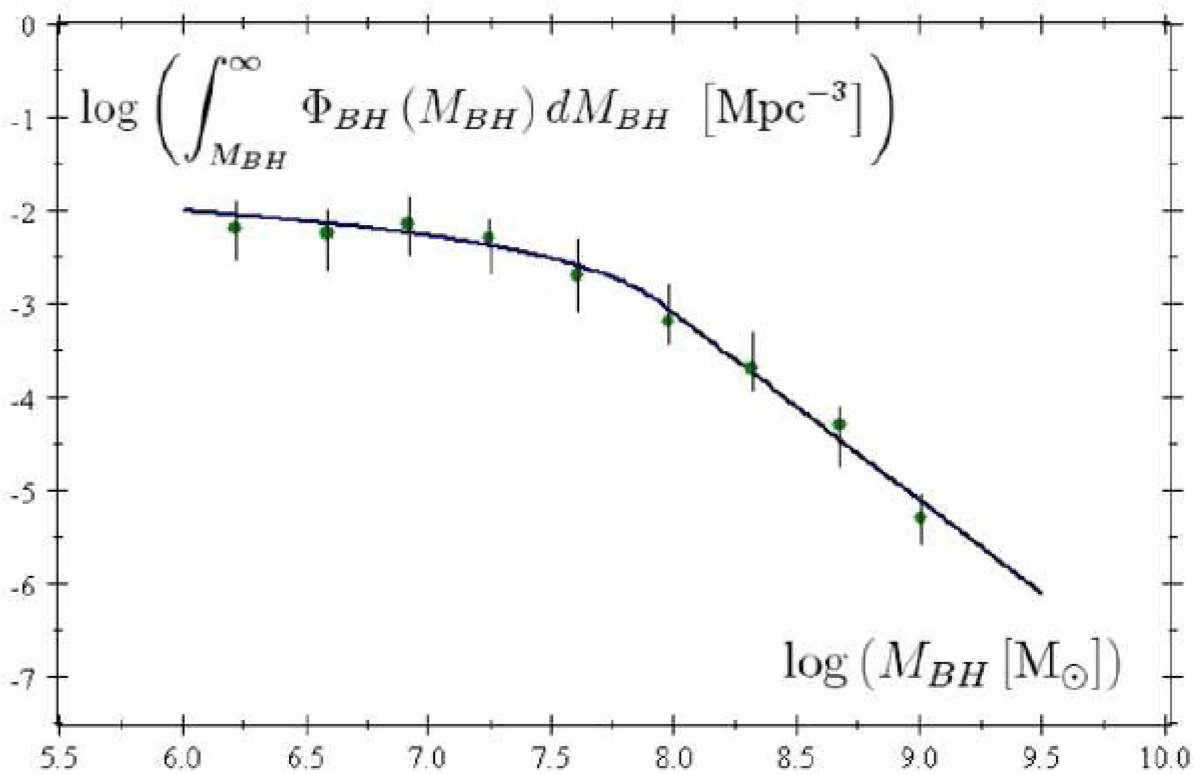

L. Á. Gergely, P. L. Biermann: [arXiv:1208.5251 [gr-qc]]

Supermassive black hole mergers

Typical mass ratios of SMBH binaries

L. Á. Gergely, P. L. Biermann, *Astrophys. J.* **697**, 1621 (2009)

- Mass distribution of central galactic BHs a broken power law
- Mass of the central massive BH scales with the (Benson et al. 2007)
  - mass of the spheroidal component,
  - total mass of a galaxy (dark matter)

  → merger rate of galaxies ≈ merger rate of the central BHs.
- The probability for a specific mass ratio is an integral over the BH mass distribution, folded with the rate to merge (depending on cross section and relative velocity of the two galaxies, the latter negligible, as the universe is not old enough for mass segregation)
- Factor of 10 in radius (10^2 in cross-section) for a factor of about 10^4 in mass

  → Cross-section $F \sim \eta^{\xi}$ with $\xi = 1/2$ as first approximation

Typical mass ratio of SMBH binaries II.

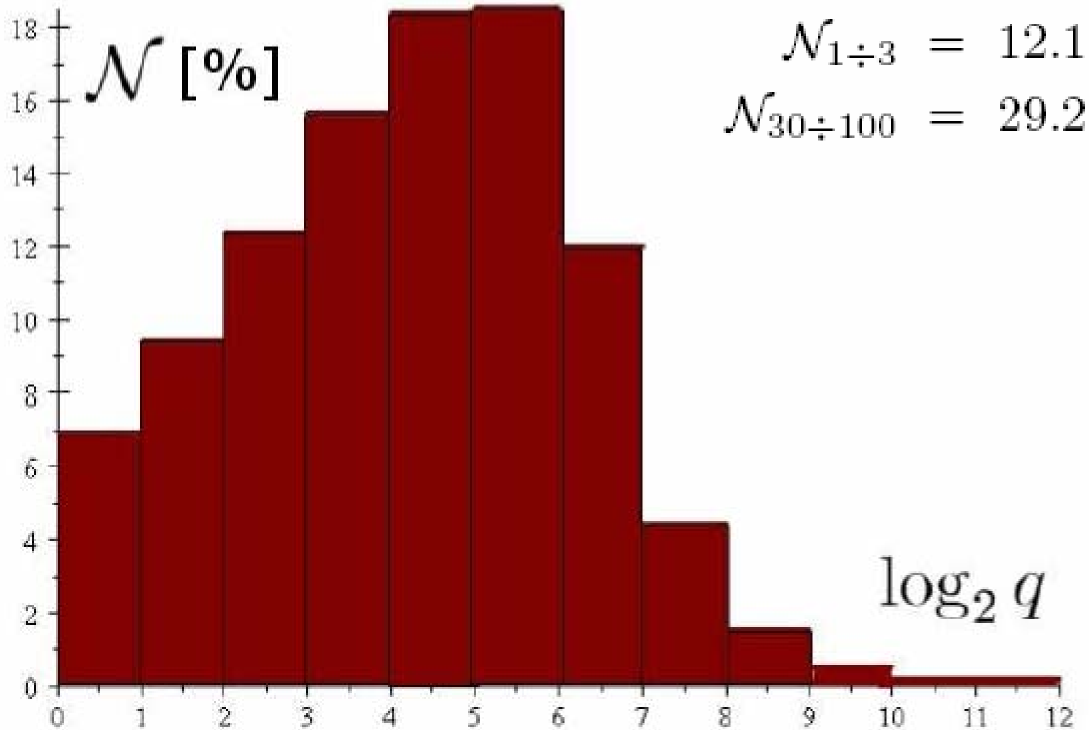

$$\mathcal{N}_{1\div 3} = 12.1\ \% , \quad \mathcal{N}_{3\div 30} = 48.9\ \% ,$$
$$\mathcal{N}_{30\div 100} = 29.2\ \%, \quad \mathcal{N}_{100\div 3000} = 9.8\ \% .$$

FIG. 2: (Color online) The number of SMBH encounters with mass ratios q as function of $\log_2 q$.

L. Á. Gergely, P. L. Biermann: [arXiv:1208.5251 [gr-qc]]

Orbital dynamics of BH binaries

Multitude of contributions to dynamics

Inspiral → merger → ringdown

PN treatment

Poisson 1998

Damour, Jaranowski Schäfer 2000

$$\mathcal{L} = \mathcal{L}_N + \mathcal{L}_{PN} + \underbrace{\mathcal{L}_{SO} + \mathcal{L}_{SS} + \mathcal{L}_{QM}}_{\text{Barker \& O'Connell 1970}} + \mathcal{L}_{2PN} + \mathcal{L}_{SOPN} + \mathcal{L}_{SSPN} + \mathcal{L}_{3PN} + \mathcal{L}_{DD}$$

$\boxed{?}$ $\boxed{?}$

Ioka & Taniguchi 2000

Damour & Deruelle 1985

Grishchuk & Kopejkin 1986

$\underbrace{\hspace{10em}}_{\text{Classical dynamics only}}$

--->
radiation losses from 2.5 PN

1. Quasi-elliptic motion. Radial motion decouples from angular motion

2. Precessional motion of the spins.

Conservative evolution (up to 2PN)

Independent variables:

1. orbital elements: [a_r (or E_N), e_r (or A_N), Euler angles ($-\phi_n$, ψ_p, α)]
2. spin angles [κ_i, ψ_i]
3. masses m_i, dimensionless spins χ_i, total angular momentum J

Keplerian orbits: all conserved

2PN orbits with SO, SS, QM: m_i, χ_i, J conserved; the rest evolve

–> system of first order ordinary differential equations

The network of angles

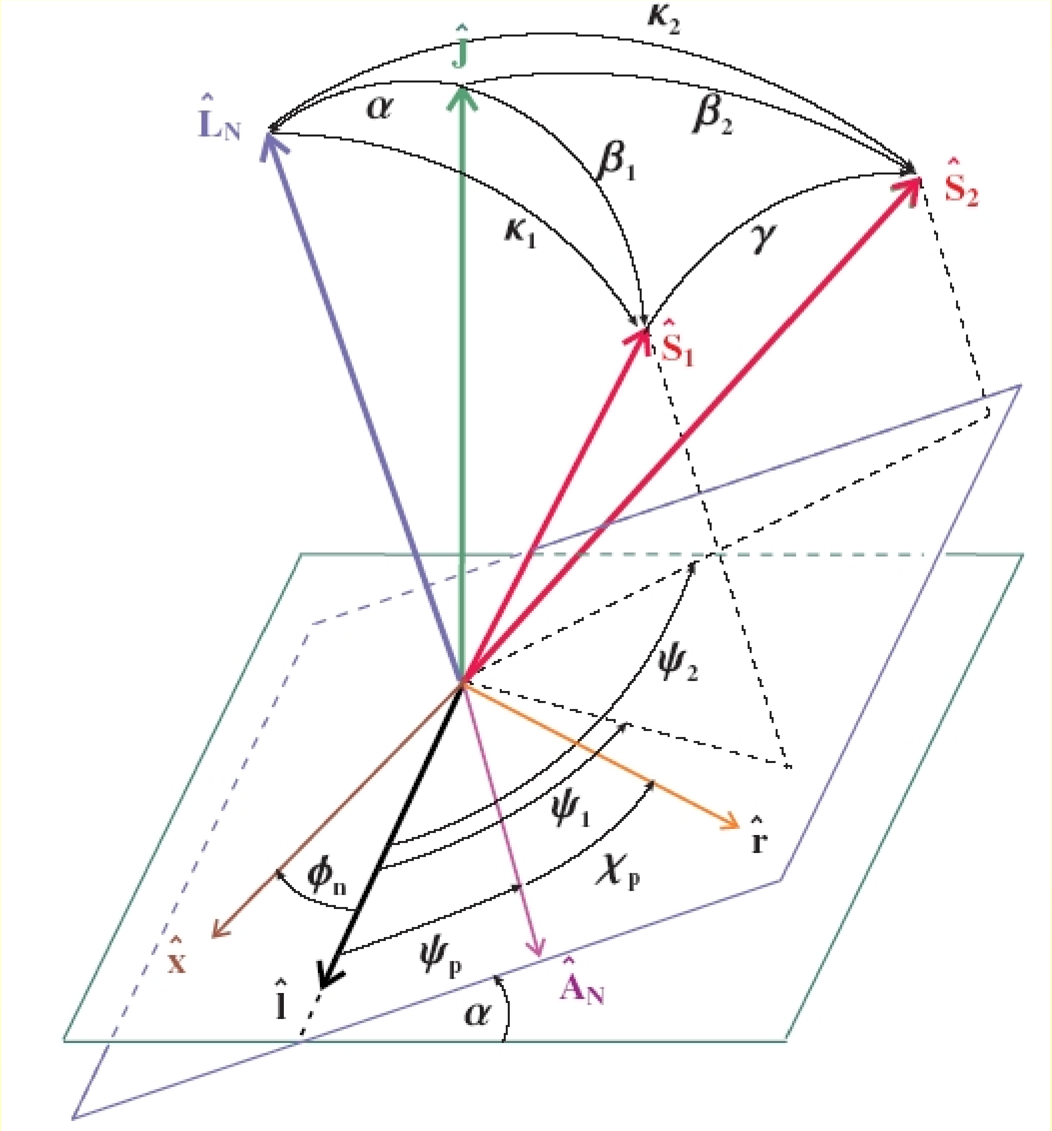

Conservative evolution II.

$$\dot{\mathfrak{l}}_r = \frac{\mathfrak{l}_r^2}{1+e_r\cos\chi_p}\left[-\left(\mathfrak{a}\cdot\hat{\mathbf{A}}_{\mathbf{N}}\right)\sin\chi_p + \left(\mathfrak{a}\cdot\hat{\mathbf{Q}}_{\mathbf{N}}\right)\cos\chi_p\right] , \tag{36}$$

$$\dot{e}_r = \frac{\mathfrak{l}_r}{1+e_r\cos\chi_p}\left[-\left(\mathfrak{a}\cdot\hat{\mathbf{A}}_{\mathbf{N}}\right)\left(e_r+\cos\chi_p\right)\sin\chi_p + \left(\mathfrak{a}\cdot\hat{\mathbf{Q}}_{\mathbf{N}}\right)\left(1+2e_r\cos\chi_p+\cos^2\chi_p\right)\right] , \tag{37}$$

$$\dot{\psi}_p = -\frac{\mathfrak{l}_r}{\left(1+e_r\cos\chi_p\right)}\left[\left(\mathfrak{a}\cdot\hat{\mathbf{L}}_{\mathbf{N}}\right)\frac{\sin\left(\psi_p+\chi_p\right)}{\tan\alpha} + \left(\mathfrak{a}\cdot\hat{\mathbf{A}}_{\mathbf{N}}\right)\frac{\left(1+e_r\cos\chi_p+\sin^2\chi_p\right)}{e_r} - \left(\mathfrak{a}\cdot\hat{\mathbf{Q}}_{\mathbf{N}}\right)\frac{\sin\chi_p\cos\chi_p}{e_r}\right] , \tag{38}$$

$$\dot{\alpha} = \mathfrak{l}_r\left(\mathfrak{a}\cdot\hat{\mathbf{L}}_{\mathbf{N}}\right)\frac{\cos\left(\psi_p+\chi_p\right)}{1+e_r\cos\chi_p} , \tag{39}$$

$$\dot{\phi}_n = -\mathfrak{l}_r\left(\mathfrak{a}\cdot\hat{\mathbf{L}}_{\mathbf{N}}\right)\frac{\sin\left(\psi_p+\chi_p\right)}{\left(1+e_r\cos\chi_p\right)\sin\alpha} , \tag{40}$$

$$\dot{\kappa}_i = -\left(\omega_{\mathbf{i}}\cdot\hat{\mathbf{A}}_{\mathbf{N}}\right)\sin\zeta_i + \left(\omega_{\mathbf{i}}\cdot\hat{\mathbf{Q}}_{\mathbf{N}}\right)\cos\zeta_i - \mathfrak{l}_r\left(\mathfrak{a}\cdot\hat{\mathbf{L}}_{\mathbf{N}}\right)\frac{\sin\left(\chi_p-\zeta_i\right)}{1+e_r\cos\chi_p} , \tag{41}$$

$$\dot{\zeta}_i = -\left[\left(\omega_{\mathbf{i}}\cdot\hat{\mathbf{A}}_{\mathbf{N}}\right)\cos\zeta_i + \left(\omega_{\mathbf{i}}\cdot\hat{\mathbf{Q}}_{\mathbf{N}}\right)\sin\zeta_i\right]\cot\kappa_i + \left(\omega_{\mathbf{i}}\cdot\hat{\mathbf{L}}_{\mathbf{N}}\right) + \frac{\mathfrak{l}_r}{\left(1+e_r\cos\chi_p\right)} \times\left[\left(\mathfrak{a}\cdot\hat{\mathbf{L}}_{\mathbf{N}}\right)\frac{\cos\left(\chi_p-\zeta_i\right)}{\tan\kappa_i} + \left(\mathfrak{a}\cdot\hat{\mathbf{A}}_{\mathbf{N}}\right)\frac{\left(1+e_r\cos\chi_p+\sin^2\chi_p\right)}{e_r} - \left(\mathfrak{a}\cdot\hat{\mathbf{Q}}_{\mathbf{N}}\right)\frac{\sin\chi_p\cos\chi_p}{e_r}\right] , \tag{42}$$

$$\dot{\chi}_p = \frac{\left(1+e_r\cos\chi_p\right)^2}{\mathfrak{l}_r^3} + \frac{\mathfrak{l}_r}{e_r\left(1+e_r\cos\chi_p\right)} \times\left[\left(\mathfrak{a}\cdot\hat{\mathbf{A}}_{\mathbf{N}}\right)\left(1+e_r\cos\chi_p+\sin^2\chi_p\right) - \left(\mathfrak{a}\cdot\hat{\mathbf{Q}}_{\mathbf{N}}\right)\sin\chi_p\cos\chi_p\right] . \tag{43}$$

L. Á. Gergely: *Phys. Rev.* D 81, 084025 (2010)
L. Á. Gergely: *Phys. Rev.* D 82, 104031 (2010)

Gravitational radiation from BH binaries

GW detection from binaries

LIGO, VIRGO worked, GEO workes at designed sensitivity (40– 2000 Hz)

by 2015 advanced LIGO, VIRGO

2023+ (e)LISA (10^{-5} - 1 Hz)

Other projects: Large Scale Cryogenic Gravitational Wave Telescope (LCGT), Einstein Telescope (ET)

GW= combination of 2 polarizations: **+ x** , weighted by antenna functions (depending on source location)

What had LIGO/Virgo not heard yet?

$f_{wave} = \frac{c^3}{6^{3/2}\pi G M_\odot}\left(\frac{m}{M_\odot}\right)^{-1}$
$m_{f_{wave}=2000\ \mathrm{Hz}} = 2.19\, M_\odot$
$m_{f_{wave}=600\ \mathrm{Hz}} = 7.31\, M_\odot$
$m_{f_{wave}=80\ \mathrm{Hz}} = 54.97\, M_\odot$
$m_{f_{wave}=50\ \mathrm{Hz}} = 87.94\, M_\odot$

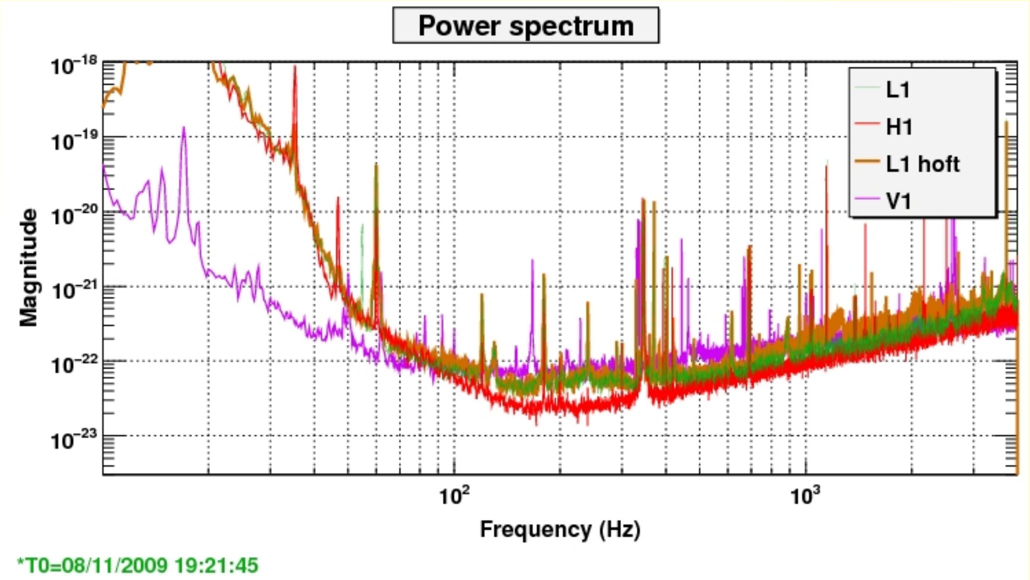

Neutron stars, stellar size BHs

Two black holes, each of 2 ½ solar masses

Scott Hughes,

http://web.mit.edu/sahughes/www/sounds.html

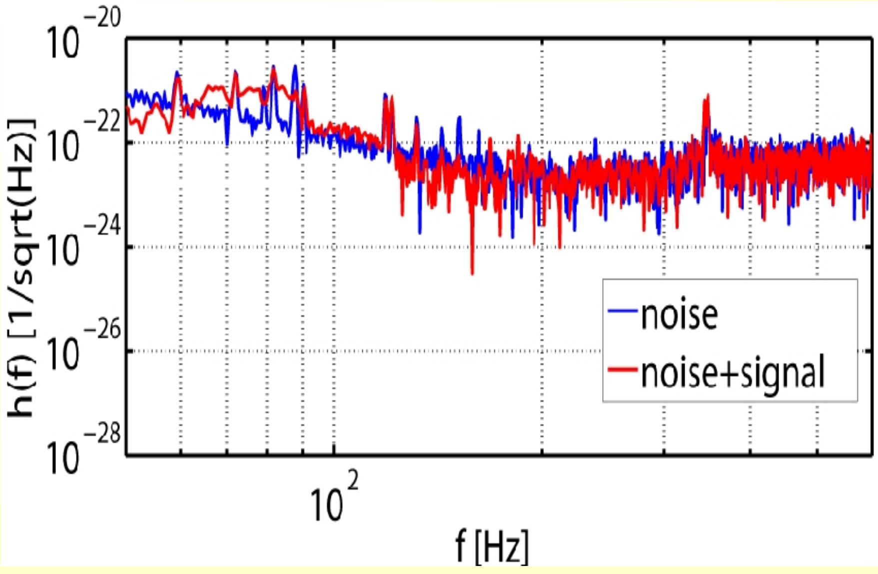

Earthquakes, storms and waves

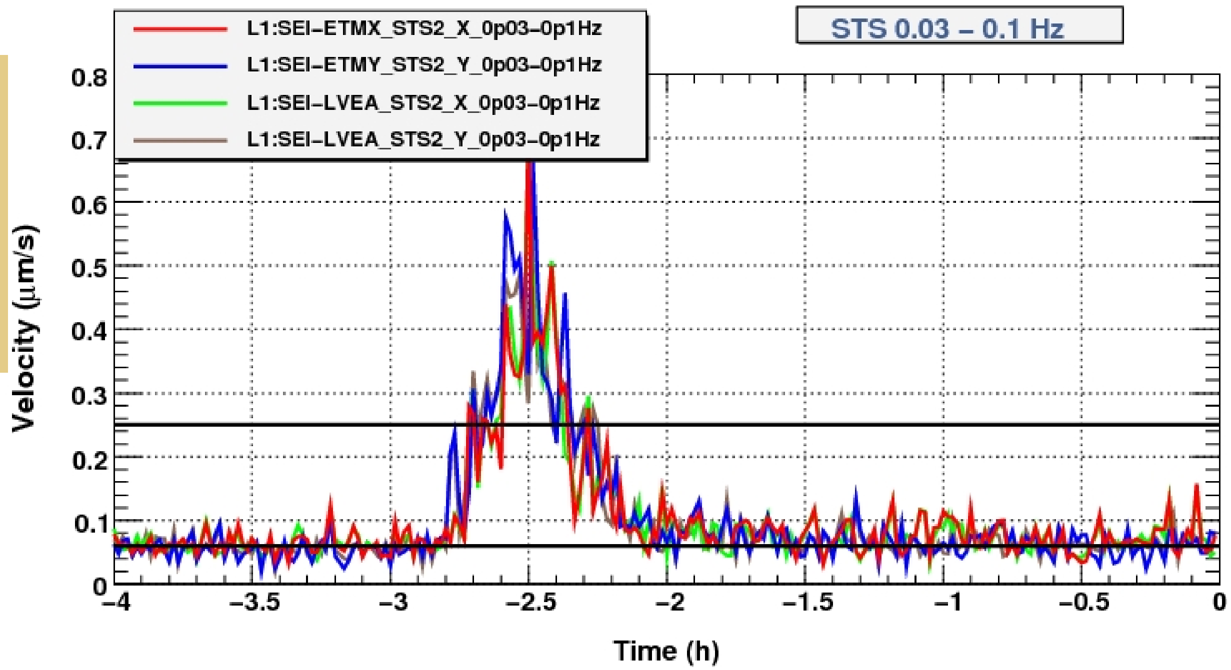

large sensitivity = large instability

Costa Rica earthquake 4.9 Richter scale, November 2009

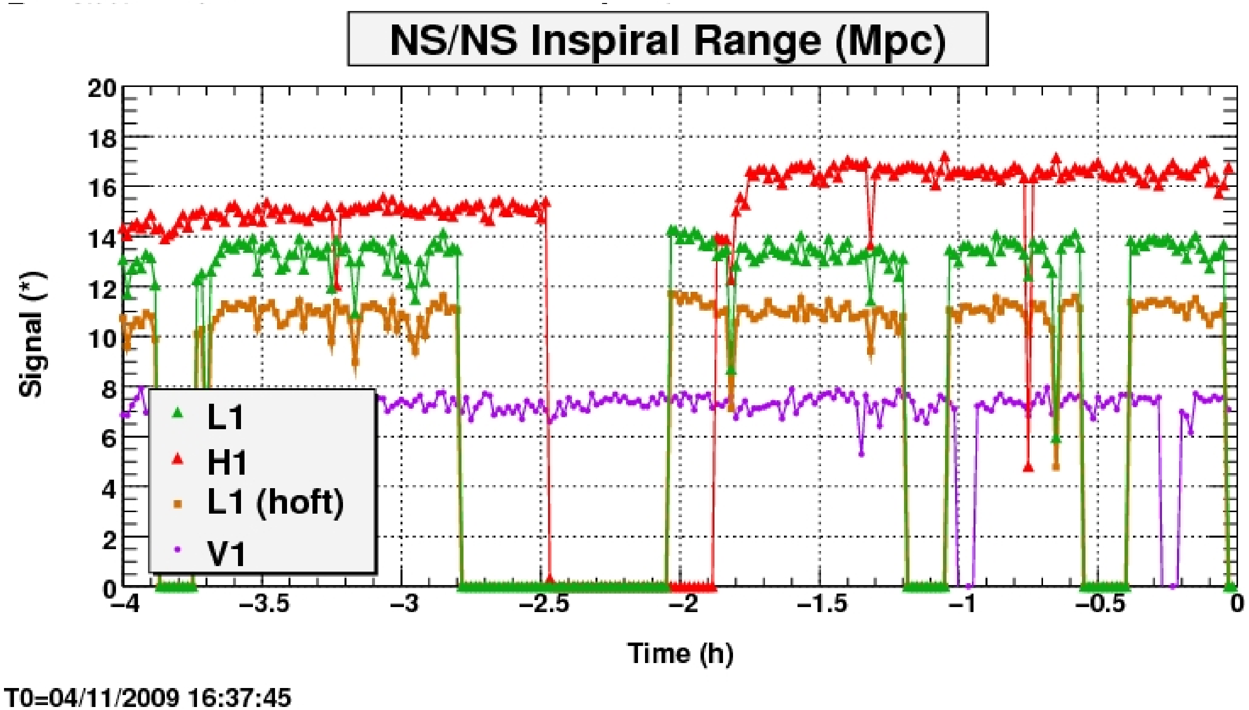

Need for active seismic isolation: advanced LIGO will have

Gravitational waves in the LIGO/Virgo frequency band

non-spinning signals | spinning signals $\chi_{1,2}$>.9

(other parameters kept the same)

M1=5.20   M2=3.81

M1=3.55   M2= 3.35

M1=6.43   M2=3.09

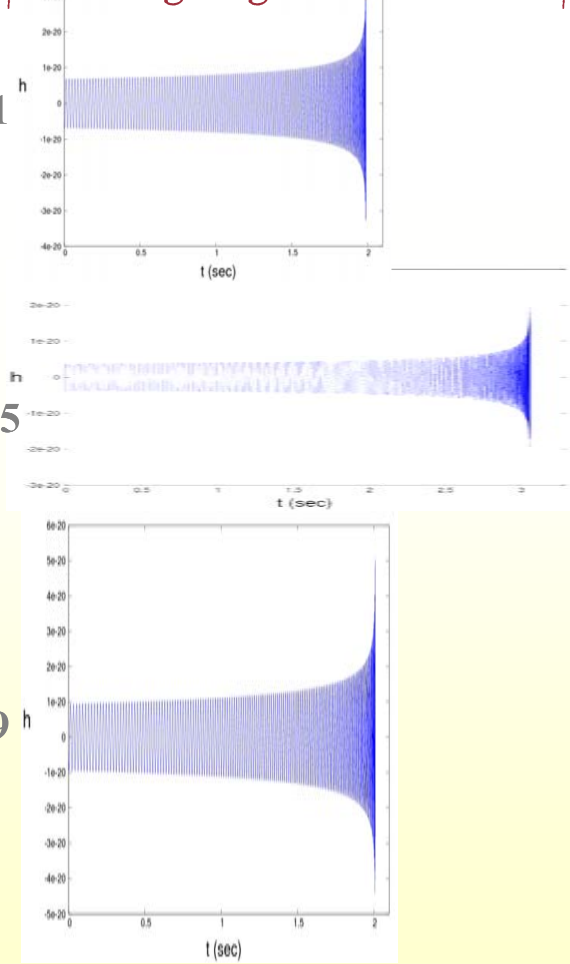

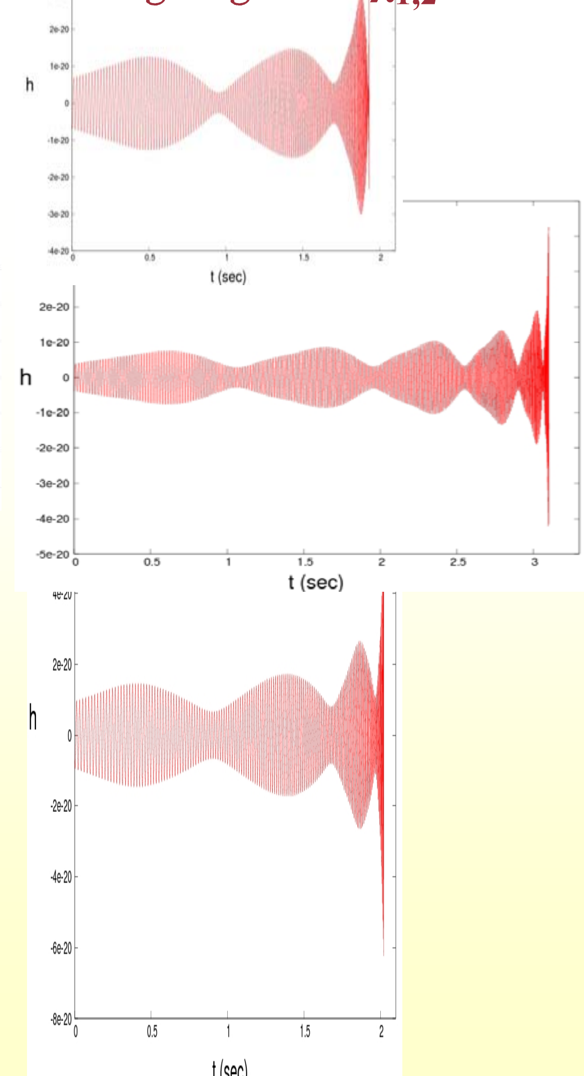

→ Amplitude modulation by spins

More accurate waveforms: equal mass

spin-orbit

spin-spin

self-spin
and
quadrupole-
monopole
corrections

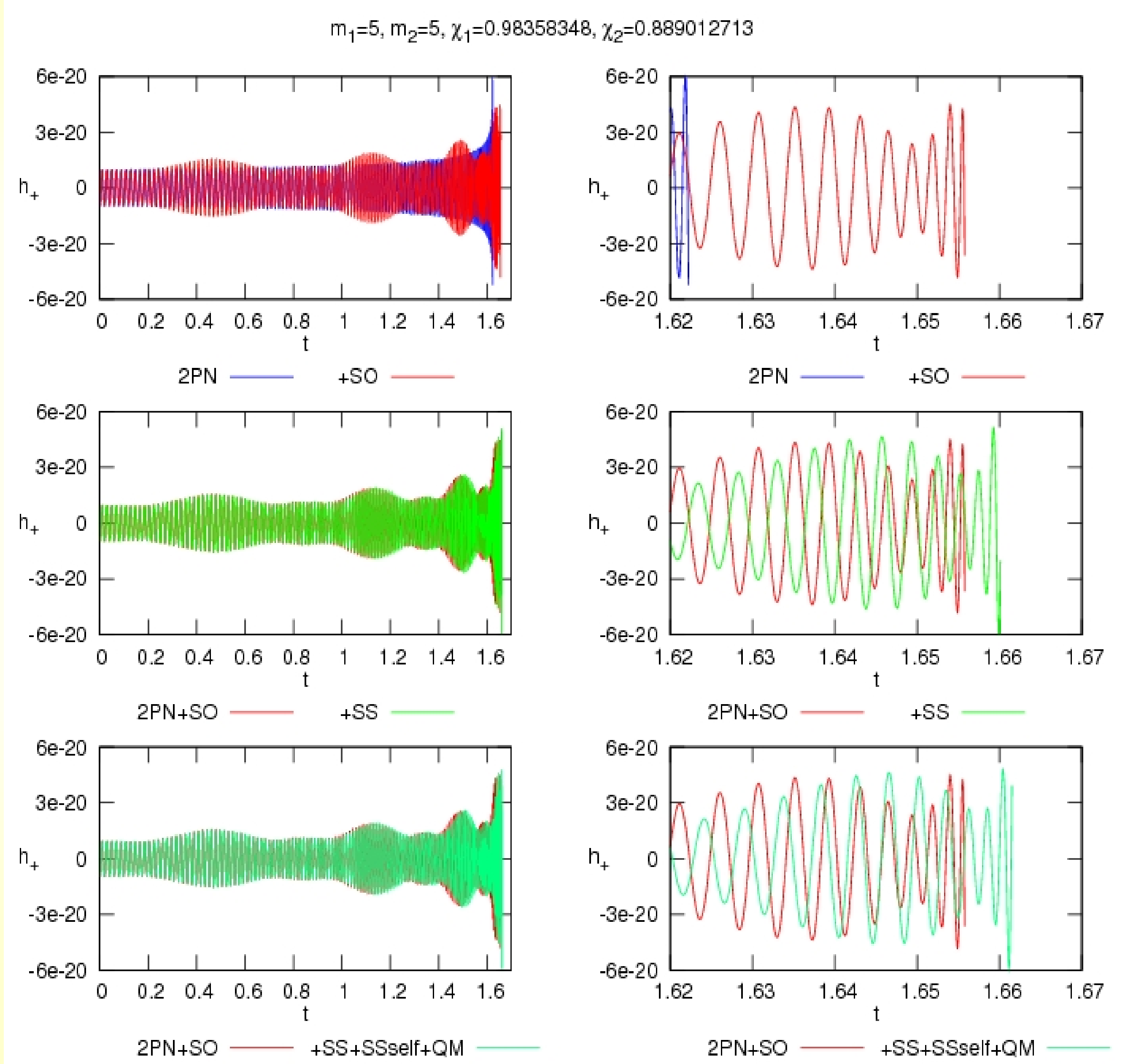

More accurate WFs: unequal mass

mass ratio
$\nu=0.1$

spin-orbit

spin-spin

self-spin
and
quadrupole-
monopole
corrections

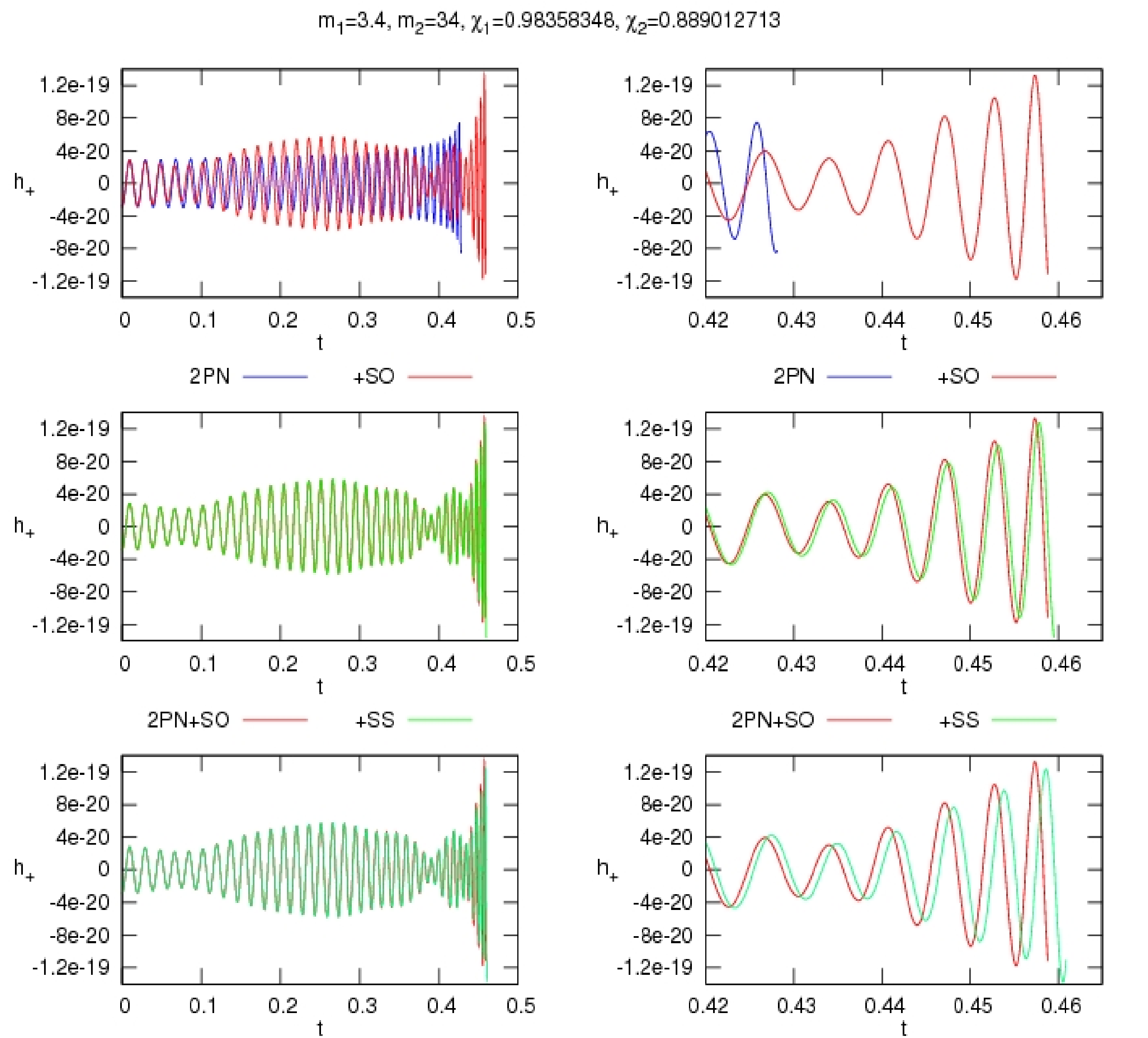

Supermassive black hole binaries

$$f_{wave} = \frac{c^3}{6^{3/2}\pi G M_\odot}\left(\frac{m}{M_\odot}\right)^{-1}$$

x (1+z) redshift dependence

$$m_{f_{wave}=10^{-5}\ \mathrm{Hz}} = 4.38 \times 10^8 \, M_\odot$$

SMBHs in the middle mass range

$$m_{f_{wave}=1\ \mathrm{Hz}} = 4380 \, M_\odot$$

Intermediate Mass BH:
do they exist?

Possibility to test cosmological models with them:
amplitude (waveform) & phase of GWs

- can be measured independently
- have different redshift-dependence

The sound of LISA:

Initially highly eccentric orbit, into rapidly spinning black hole

Initially circular orbit, into rapidly spinning black hole

Scott Hughes, http://web.mit.edu/sahughes/www/sounds.html

Parameter estimation of GW sources

2 masses

2 spin magnitudes

4 spin angles

3 params for sky location and luminosity distance

2 params for the orientation of the orbit w.r. to the line of sight

1 param: the GW phase at some initial measurement time

2 params: relative orientation of the detector w.r. to the line of sight

→ 16 params, with strong degeneracies !!!

Parameter estimation by Markoff-Monte Carlo chains of several million steps, converging slowly even on supercomputers, in several weeks, if at all

Parameter estimation of GW sources - an example

The effects of LIGO detector noise on a 15-dimensional Markov-chain Monte-Carlo analysis of gravitational-wave signals

V. Raymond[1], M.V. van der Sluys[2], I. Mandel[1], V. Kalogera[1], C. Röver[3], N. Christensen[4]

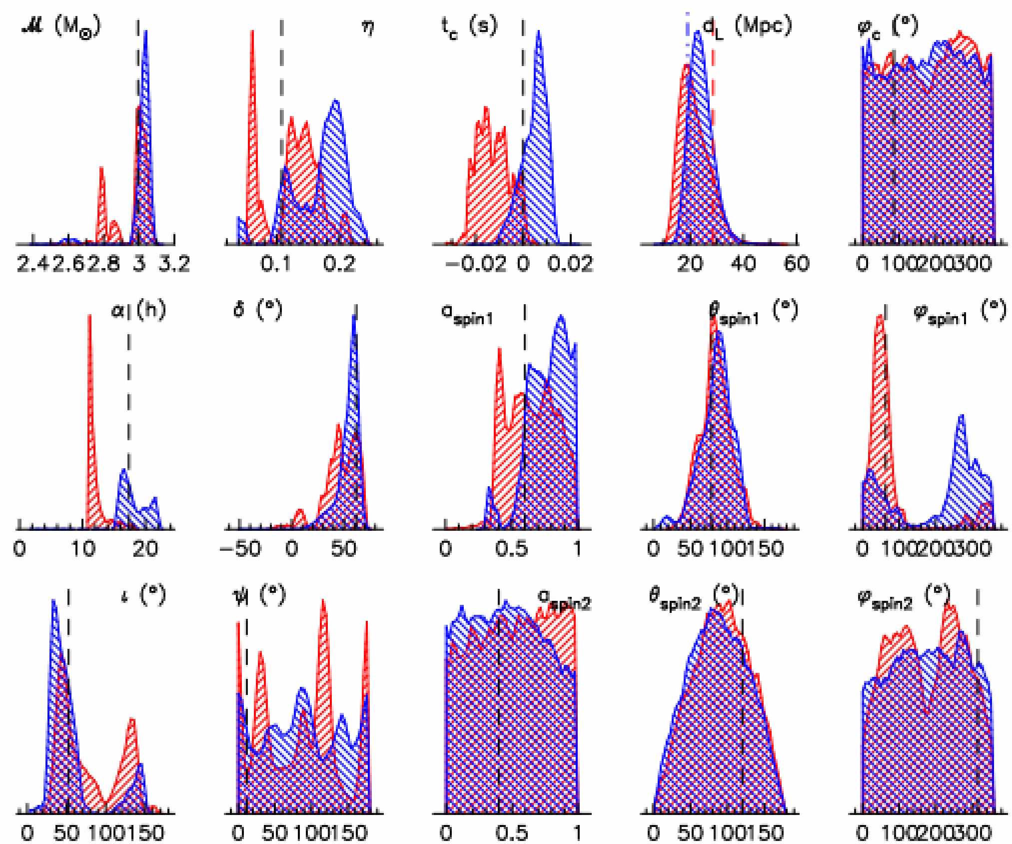

Figure 1: One-dimensional marginalised PDFs for all 15 parameters from our analysis of data sets DS1 (hatched upward; red in the online colour version) and DS2 (hatched downward; blue in the online colour version). The vertical dashed lines mark the injection values.

Typical mass ratios

consequence 1:

typical spin in LISA mergers

Final spin in LISA mergers

Final spin derived from PN arguments
- for the typical unequal masses matches quite well the numerical formula of
E. Barausse, L. Rezzolla, *Astrophys. J. Lett* **704**, L40-L44 (2009)

$$\chi_f = \frac{\nu}{(1+\nu)^2}\left[4 + 4\sum_{i=1,2}\nu^{2i-3}\chi_i\cos\kappa_i + \sum_{i=1,2}\left(\nu^{2i-3}\chi_i\right)^2 + 2\chi_1\chi_2\cos\gamma\right]^{1/2}$$

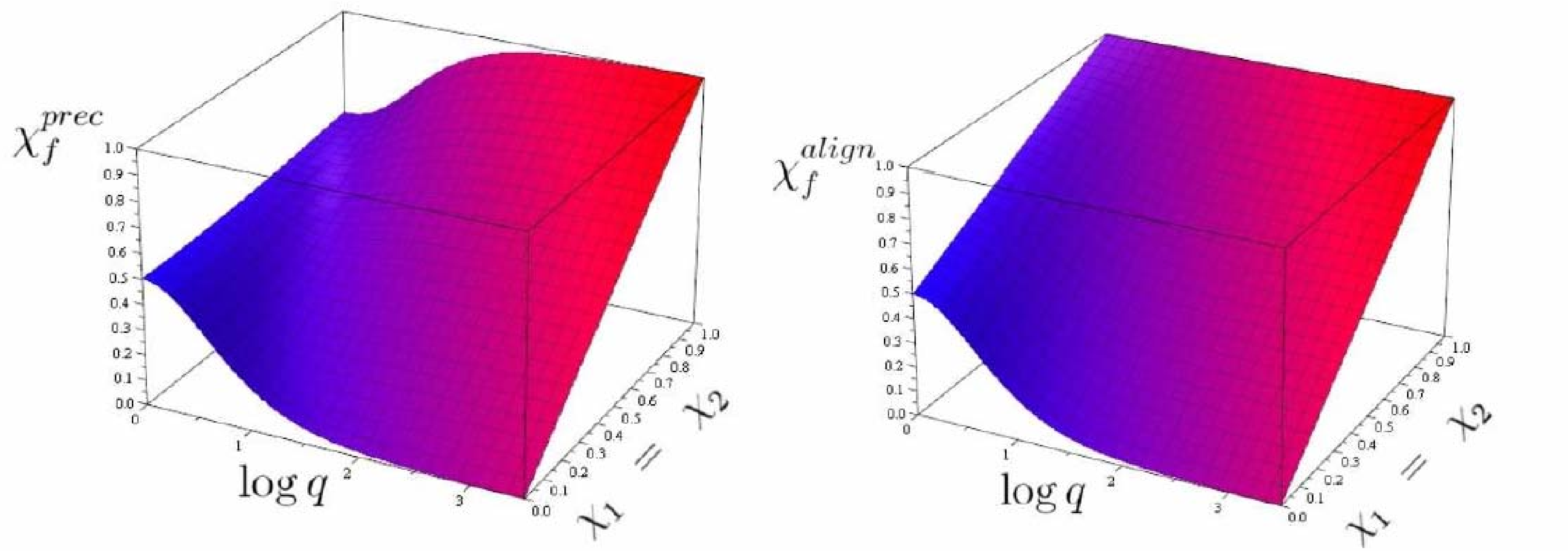

FIG. 3: (Color online) The typical final spin in supermassive black hole mergers as function of $\chi_1 = \chi_2$ and $\log q$, represented for precessing mergers (averaged over random configurations) - left panel; and mergers with the spins and orbital angular momentum fully aligned - right panel.

integral over configurations

L. Á. Gergely, P. L. Biermann: [arXiv:1208.5251 [gr-qc]]

Typical spin in LISA mergers

further integral over mass ratios, weighted by the mass ratio probability

L. Á. Gergely, P. L. Biermann:

[arXiv:1208.5251 [gr-qc]]

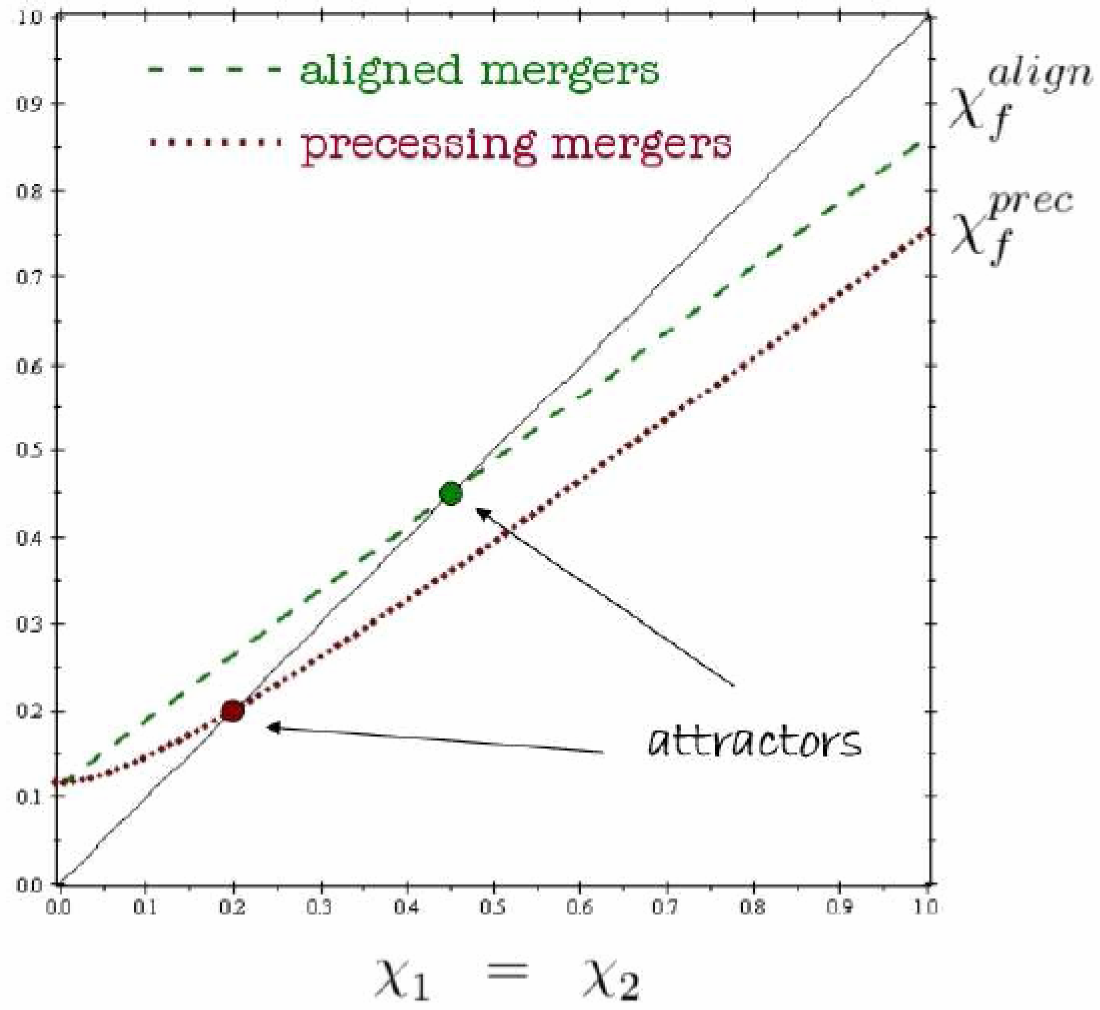

FIG. 4: (Color online) The typical final spin χ_f as function of $\chi_1 = \chi_2$ only, in the randomly precessing and the non-precessing merger limits (lower and upper curves, re-

But: BHs will spin-up due to accretion

Bardeen accretion spins up BHs.

Mass increase by a factor of 3, when changing BHs spin from maximal counter-rotation to maximal rotation.

Efficiency of accreted rest mass conversion into outgoing electromagnetic radiation is 42.3%.

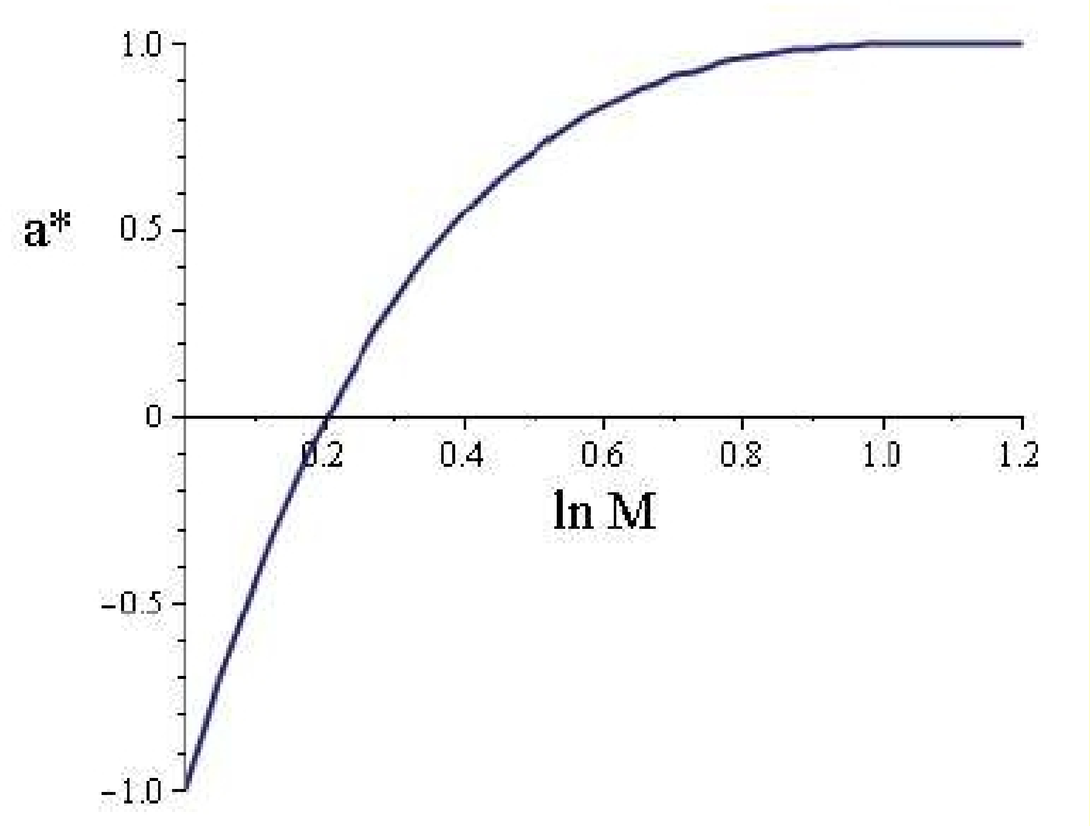

Symbiotic system of BH, accretion disk, magnetic fields, jets

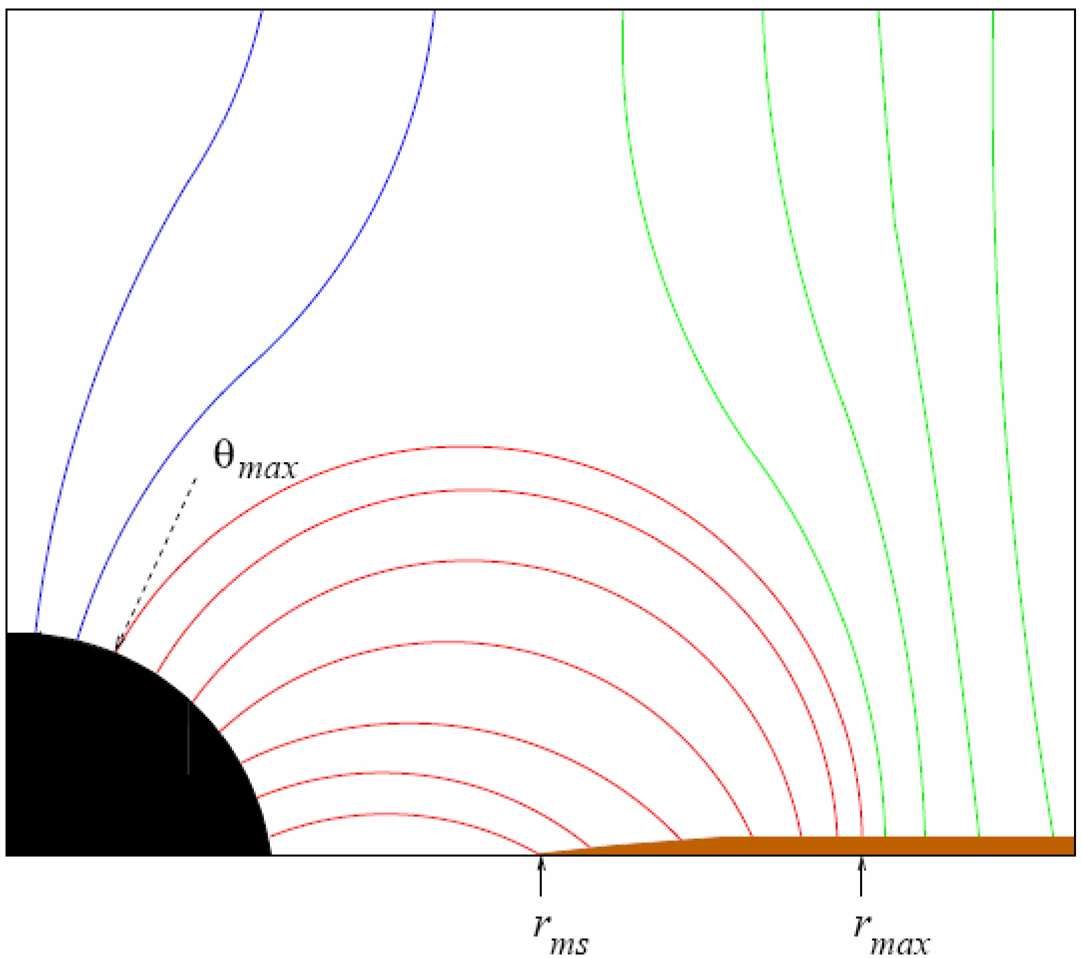

Figure 2. The open and closed magnetic field line topology.

Lots of auxiliary information from the BH environment

Accretion and efficiency refined

Corrections from:

- photon capture
- open magnetic fields
- inner truncation of the disk radiation due to a jet

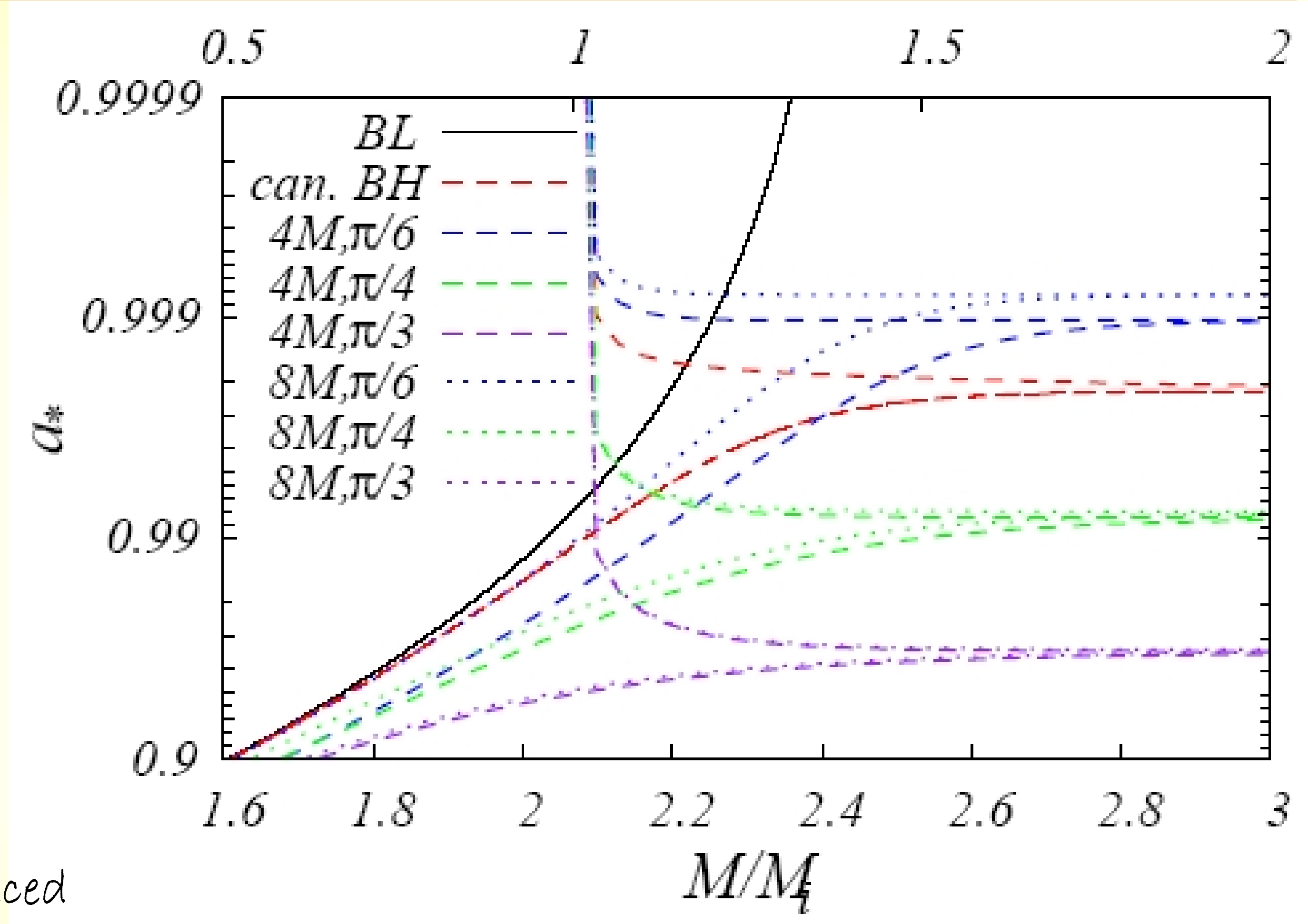

Spin limit

slightly reduced

Efficiency reduced to 25% - 35 %

Z Kovács, LÁ Gergely, PL Biermann: Mon. Not. Royal Astron. Soc. **416**, 991 (2011)

Typical mass ratios consequence 2: spin-flip and X-shaped radio galaxies

End of inspiral: the spin dominates

Table 1. The evolution of the ratio $S_1/L \approx \varepsilon^{1/2}\eta^{-1}$ in the range $\varepsilon = 10^{-3} \div 10^{-1}$ for various values of the mass ratio η.

$S_1/L = \varepsilon^{1/2}\eta^{-1}$	$\varepsilon \approx 10^{-3}$		$\varepsilon \approx 10^{-1}$	
$\eta = 1$	0.03	$(S_1 \ll L)$	0.3	$(S_1 < L)$
$\eta = 1/3$	0.1	$(S_1 < L)$	1	$(S_1 \approx L)$
$\eta = 1/30$	1	$(S_1 \approx L)$	10	$(S_1 > L)$
$\eta = 1/900$	30	$(S_1 \gg L)$	300	$(S_1 \gg L)$

Typical mass ratio 1/30÷1/3

→ ***S_1/L*** changes during the inspiral from <<1 to >>1

The dominant spin flips

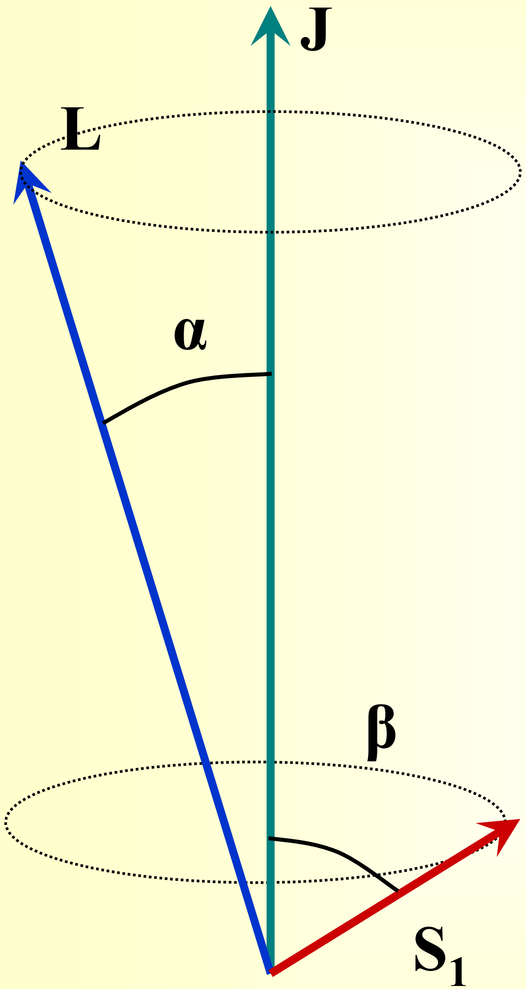

- due to GW emission the spin aligns to the original **J** direction

L. Á. Gergely, P. L. Biermann, *Astrophys. J.* **697**, 1621 (2009)

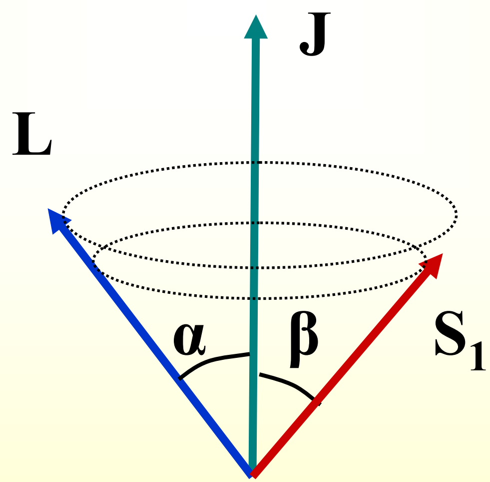

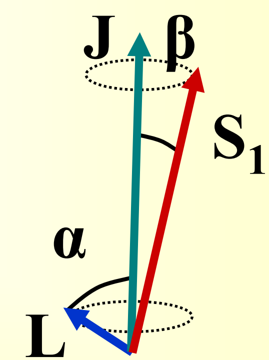

Key elements: (i) typically the BHs are not equal mass, $m_2 << m_1$, neglect $S_2 \sim m_2^2$

(ii) the direction of **J** is conserved, (iii) the magnitude of $\mathbf{S_1}$ is conserved → spin-flip

Time-scales

Table 2: Order of magnitude estimates for the inspiral rate $\dot{L}/L$, angular precessional velocity Ω_p and tilt velocity $\dot{\alpha}$ of the vectors $\mathbf{L}$ and $\mathbf{S_1}$ with respect to $\mathbf{J}$, represented for the three regimes with $L > S_1$, $L \approx S_1$ and $L < S_1$, characteristic in the domain of mass ratios $\nu = 0.3 \div 0.03$. The numbers in brackets represent inverse time scales in seconds^{-1}, calculated for the typical mass ratio $\nu = 10^{-1}$, post-Newtonian parameter 10^{-3}, 10^{-2} and 10^{-1}, respectively and $m = 10^8 M_{\odot}$ (then $c^3/Gm = 2\times 10^{-3}$ s^{-1}).

	$L > S_1$		$L \approx S_1$		$L < S_1$	
$-\dot{L}/L$	$\frac{32c^3}{5Gm}\varepsilon^4\eta$	$(\approx 10^{-15})$	$\frac{32c^3}{5Gm}\varepsilon^4\eta$	$(\approx 10^{-11})$	$\frac{32c^3}{5Gm}\varepsilon^4\eta$	$(\approx 10^{-7})$
Ω_p	$\frac{2c^3}{Gm}\varepsilon^{5/2}\eta$	$(\approx 10^{-11})$	$\frac{2c^3}{Gm}\varepsilon^{5/2}\eta\frac{J}{L}$	$\left(\approx 10^{-8}\frac{J}{L}\right)$	$\frac{2c^3}{Gm}\varepsilon^3$	$(\approx 10^{-5})$
$\frac{\dot{\alpha}}{\sin(\alpha+\beta)}$	$\frac{32c^3}{5Gm}\varepsilon^{9/2}\frac{\eta}{\nu}$	$(\approx 10^{-16})$	$\frac{32c^3}{5Gm}\varepsilon^{9/2}\frac{\eta}{\nu}\frac{L^2}{J^2}$	$\left(\approx 10^{-11}\frac{L^2}{J^2}\right)$	$\frac{32c^3}{5Gm}\varepsilon^{7/2}\eta\nu$	$(\approx 10^{-8})$

	$L > S_1$	$L \approx S_1$	$L < S_1$
Time to merger:	30 million years	300 years	few months
Precession time scale:	3000 years	3 years	days
Variation of the tilt angle during one precession:	2 arcsec (6×10^{-4} arcsec/year)		3 arcmin (/day)

How large is the spin-flip ?

$$\tan\alpha \approx \frac{\sin(\alpha+\beta)}{\chi_1^{-1}\varepsilon^{-1/2}\nu + \cos(\alpha+\beta)}$$

For an initial configuration of 0.005 pc (such that $\varepsilon \equiv \varepsilon^* = 10^{-3}$) and mass ratio $\nu = 10^{-1}$, the initial misalignment between $\mathbf{L}$ and $\mathbf{J}$ is $\alpha_{initial} \approx 18°,\ 10°,\ 0°$ for the dominant spin in the plane of orbit, spanning 45° degrees with the plane of orbit and perpendicular to the plane of orbit (such that $\alpha + \beta = 90°,\ 45°,\ 0°$), respectively. Then $\beta_{initial} = 72°,\ 35°,\ 0°$. For the same mass ratio and relative configurations, the angle α at the end of the PN epoch (at $\varepsilon = 10^{-1}$) becomes $\alpha_{final} \approx 73°,\ 35°,\ 0°$, respectively. This can be translated into a misalignment between $\mathbf{S_1}$ and $\mathbf{J}$ of $\beta_{final} = 17°,\ 10°,\ 0°$, and a spin-flip of $\Delta\beta = 55°,\ 25°,\ 0°$, respectively.

Depends on configuration

In the majority of cases it happens during the inspiral!

L. Á. Gergely,
P. L. Biermann,
L. I. Caramete:
Class. Quantum Grav. 27 194009 (2010)

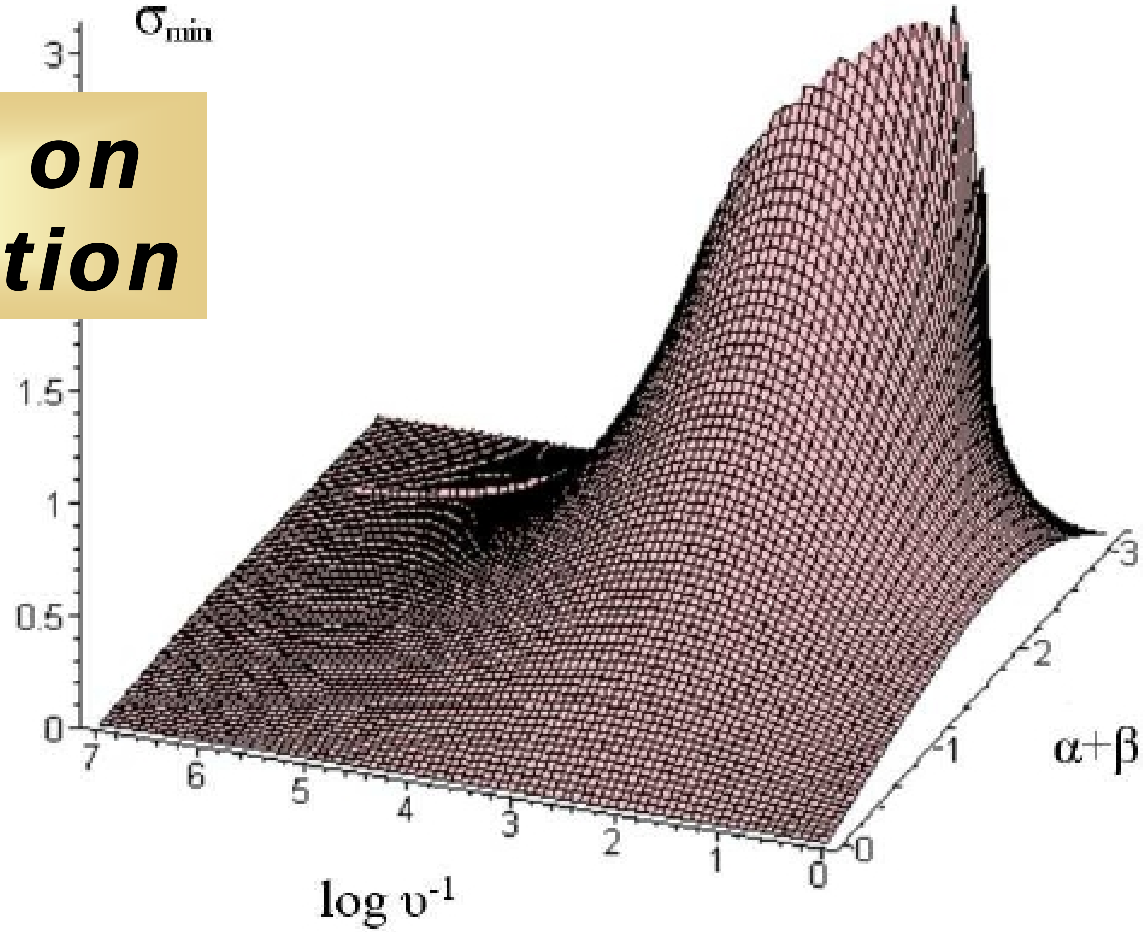

Figure 2. The spin-flip angle $\sigma_{\rm min}$ as function of the relative orientation of the spin and orbital angular momentum $\alpha+\beta$ (a constant during inspiral), and mass ratio ν. For a given mass ratio the spin-flip angle has a maximum shifted from $\pi/2$ towards the anti-aligned configurations. The mass ratios $\nu = 1;\ 1/3;\ 1/30$ and $1/1000$ are located on the $\log\nu^{-1}$ axis at 0; 1.09; 3.40 and 6.91, respectively, confirming the prediction, that a significant spin-flip will happen in the mass ratio range $\nu \in (1/30, 1/3)$. For mass ratios smaller than 1/100 the spin does not flip at all, as the infalling SMBH acts as a test particle.

XRG-catalog

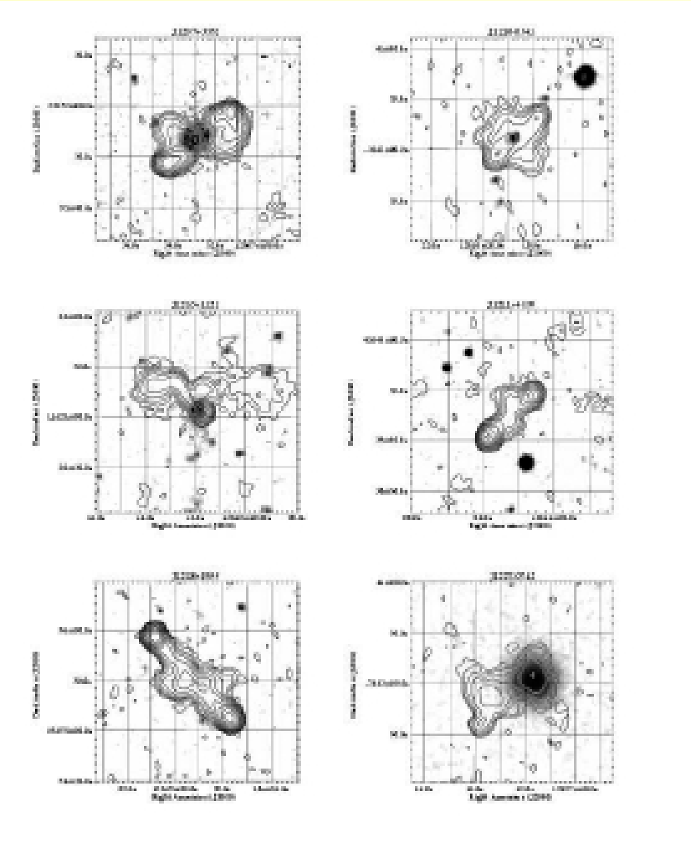

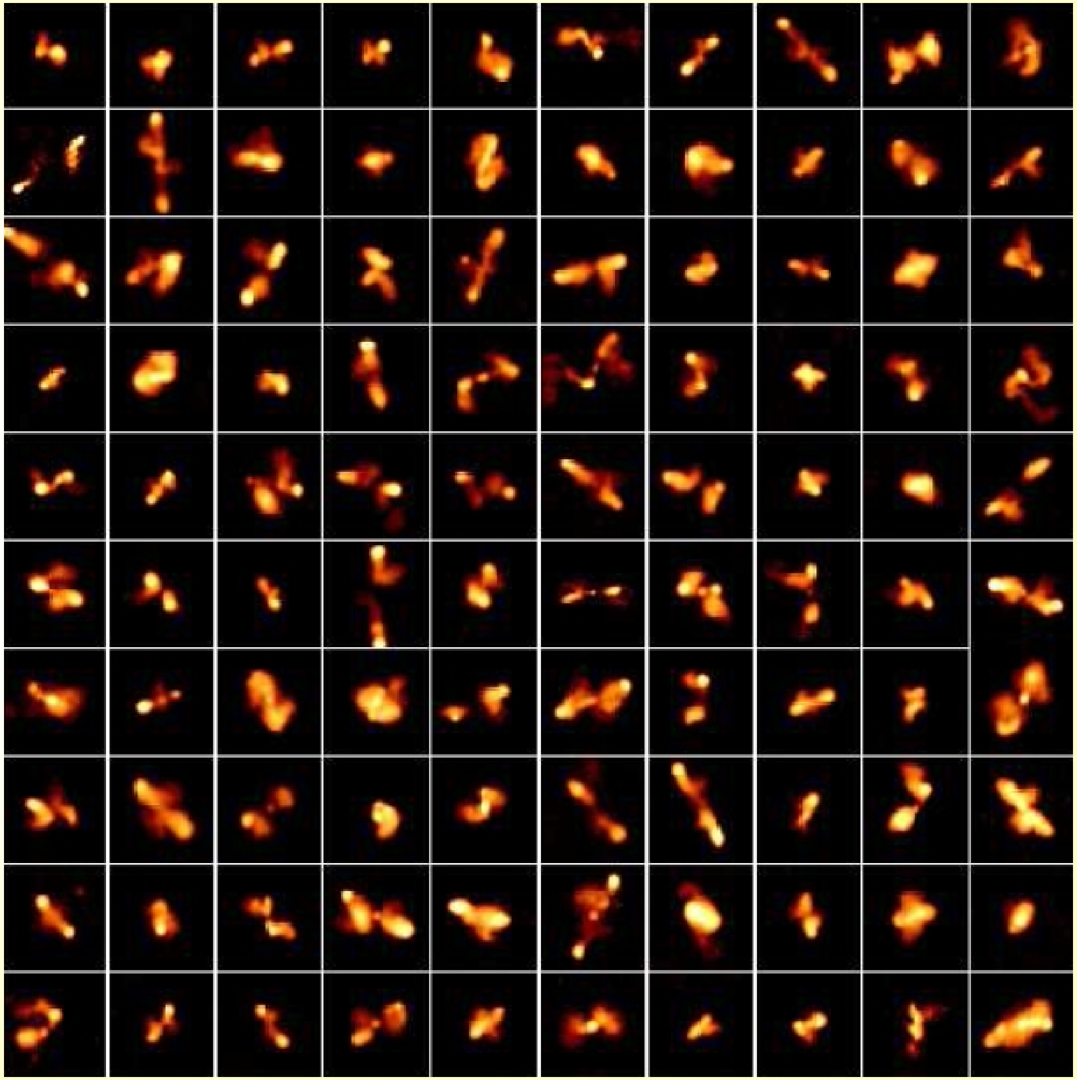

Cheung, C. C. :The Astronomical Journal, 133, 2097-2121 (2007), arXiv:astro-ph/0701278v3

Explanations

1. Galaxy harbouring twin AGNs
2. Back-flow diversion models
3. **Rapid jet reorientation (spin-flip) models**
4. Jet-shell interaction model

Need to decide case-by-case, but the spin-flip model can explain most of the observations (except possible alignment of the jets with the principal axes of the host elliptical, then 4. can)

Gopal-Krishna, PL Biermann, LÁ Gergely, PJ Wiita, *Res.Astron.Astrophys.* **12** 127 (2012)

Independent support for the spin-flip model: 31 XRGs compared to a control sample of 39 RGs with normal morphologies but similar redshifts, radio and optical luminosities

M Mezcua, AP Lobanov, VH Chavushyan, J Leon-Tavares, *Astron.Astrophys.* **527** A38 (2011)

→ members of the XRG sample: higher BH masses + older starbursts than do those of the control sample (support for merger)

Combined EM, particle physics and GW measurements

Jet variability due to precession

The narrowing of the precession cone will cause variability (flares) in the jet for a limited time

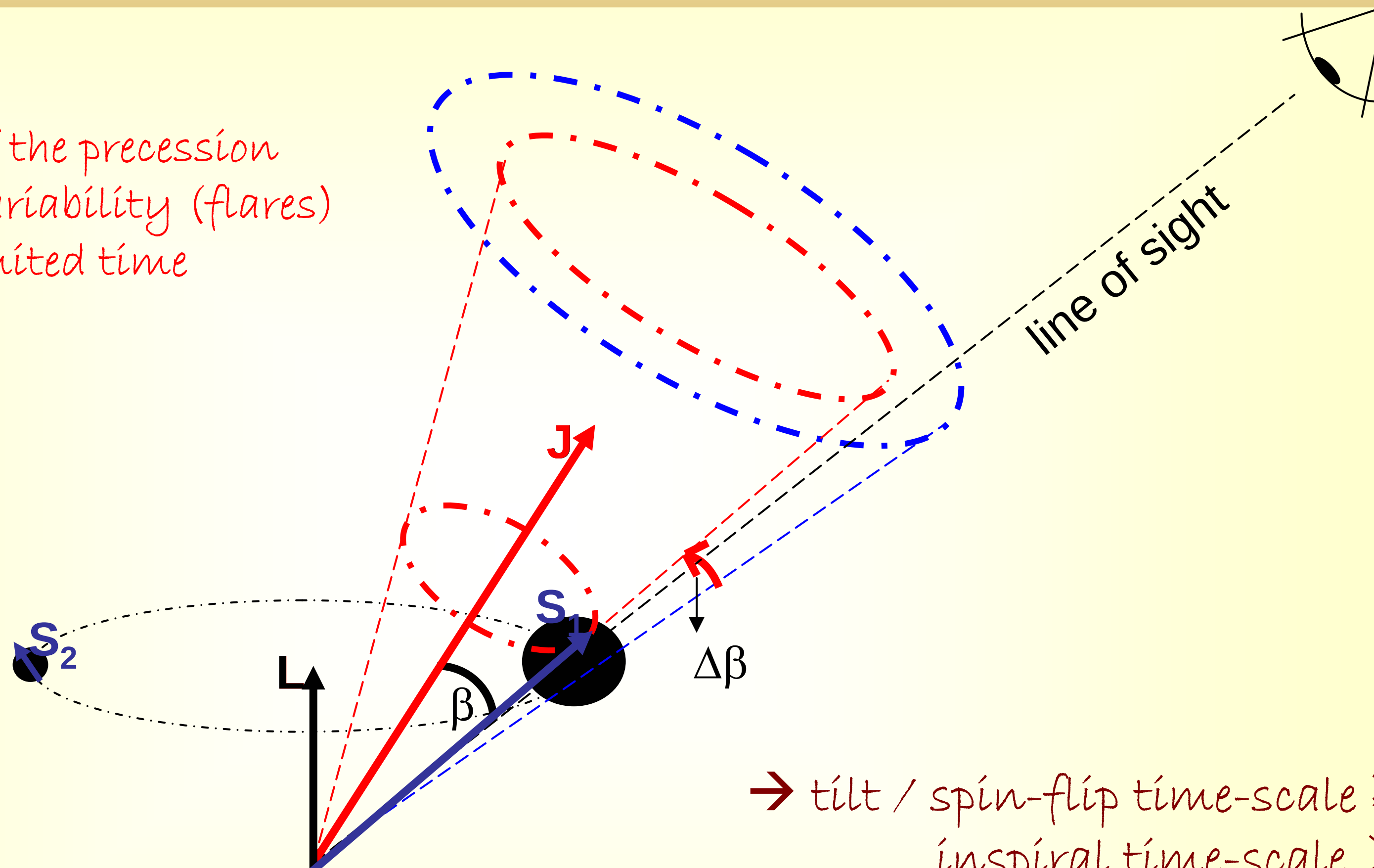

Jet measurements: source location + two time intervals → help in reconstructing the parameters of the binary

→ tilt / spin-flip time-scale ≳ inspiral time-scale ≫ precession time-scale ≫ orbital time-scale

→ E.M. counterparts to the strongest GW emission likely !!!

M. Tápai, L. Á. Gergely, Z. Keresztes, P. J. Wiita, Gopal-Krishna, P. L. Biermann: *Proceedings of the 6th Workshop of Young Researchers in Astronomy and Astrophysics on The Multi-wavelength Universe - from Starbirth to Star Death*, Budapest, Hungary (2012)

Jet variability due to precession II.

Time intervals to be observed:

- precession period of S_1 :

$$T_p(\varepsilon, \nu, f_{GW}, \beta) = \frac{(1+\nu)^2}{\varepsilon\nu} \frac{\sin\beta}{\sin\kappa} f_{GW}^{-1}$$

- time the jet spends in $\Delta\beta$:

$$T_{\Delta\beta}(\varepsilon, \nu, f_{GW}, \beta, \Delta\beta) = \frac{5\Delta\beta}{32\pi} \frac{(1+\nu)^2 \sin\kappa}{\varepsilon^3 \sin^2\beta} f_{GW}^{-1}$$

- Their ratio:

$$\frac{T_{\Delta\beta}}{T_p}(\varepsilon, \nu, \beta; \Delta\beta) = \frac{5\Delta\beta}{32\pi} \frac{\nu \sin^2\kappa}{\varepsilon^2 \sin^3\beta}$$

, where $\kappa = \alpha + \beta$, obeying

$$\kappa = \beta + \arcsin\left[\varepsilon^{1/2}\nu^{-1}\sin\beta\right]$$

For given ν and β + observed T_p and $T_{\Delta\beta}$ we can calculate $\varepsilon_{\Delta\beta}$ and f_{gw} (or m, according to

$$f_{GW} = \frac{c^3}{\pi G m}\varepsilon^{3/2}$$

).

For sources with $m = 10^6 M_\odot$, $\varepsilon_{\Delta\beta} = 0.1$, and $\nu = 0.1$ the values of T_p and $T_{\Delta\beta}$, to be observed are

β [°]	κ [°]	T_p [days]	$T_{\Delta\beta}$ [days]
20	40	116	1041
25	50	120	812
30	60	126	656
35	70	133	541
40	80	142	451

Jet variability acts as a beacon for GWs to be detected from the same source later on!

Complementary GW measurements

The leading order frequency domain waveform (for an averaged antenna pattern function):

$$\tilde{h}_\alpha(f) = \frac{\sqrt{3}}{2} A f^{-7/6} e^{i\psi(f)},\ \alpha = I, II$$

$$A = \frac{1}{\sqrt{30}\pi^{2/3}} \frac{m_{chirp}^{5/6}}{D_L}$$

and the LISA spectral noise density:

$$S_h(f) = S_{h,inst}(f) + S_{h,conf}(f)$$

$$S_{h,inst}(f) = 5.049 \times 10^5 \left[a^2(f) + b^2(f) + c^2\right]$$

$$a(f) = 10^{-22.79} (f/10^{-3})^{-7/3}$$

$$b(f) = 10^{-24.54} (f/10^{-3})$$

$$c = 10^{-23.04}$$

$$S_{h,conf}(f) = \begin{cases} 10^{-42.685} f^{-1.9} & f \le 10^{-3.15} \\ 10^{-60.325} f^{-7.5} & 10^{-3.15} < f \le 10^{-2.75} \\ 10^{-46.85} f^{-2.6} & 10^{-2.75} < f \end{cases}$$

(instrument and confusion noises C. Cutler, *Phys.Rev.* D **57**, 7089 (1998)

gives the signal to noise ratio (SNR):

$$SNR = \sqrt{4 \int_{f_{in}}^{f_{end}} \frac{\left|\tilde{h}(f)\right|^2}{S_h(f)} df}$$

Suppose gravitational waves are first detected following the jet flares at SNR=10, then until the merger, gives two additional time intervals. For

$\Delta\beta = 1^\circ$, $\beta = 30^\circ$, $T_{\Delta\beta} = 450$ days and $T_p = 80$ days

ν	m $[M_\odot]$	$\varepsilon_{\Delta\beta}$	ε_{SNR10}	T_{SNR10} $[days]$	T_{merger} $[days]$
1/3	2×10^6	0.0129	0.0138	97	332
1/10	0.5×10^6	0.0095	0.0113	457	458
1/20	0.2×10^6	0.0078	0.0139	1287	141
1/30	6768	0.0035	0.0065	1320	132

Combined GW & jet measurements

Jet measurements give sky location and redshift +

- precession period T_p and time-span of the variability $T_{\Delta\beta}$
- precession cone β and change of precession cone $\Delta\beta$

E. Kun, K. Gabányi, S. Britzen, Gopal-Khrisna. P. L. Biermann, L. Á. Gergely: *in preparation* (2012)

GW measurements give

- time when SNR=10 (or any reasonable other value), T_{SNR10}
- time when GW signal stops $T_{merger} \approx$ time of the inspiral

→Location , redshift + 6 measurements

GW signal expressed in terms of location, redshift + 5 astrophysical variables:

$\left\{\begin{array}{l}\text{dominant spin magnitude and} \\ \text{inclination, mass ratio,} \\ \underbrace{\text{total mass, PN parameter at emission}}_{\text{separation, GW frequency at emission}}\end{array}\right.$

L. Á. Gergely, M. Tápai, Z. Keresztes: *in preparation* (2012)

β from jets, the other 4 variables expressed as function of (T_{SNR10}, T_{merger}, T_p, $T_{\Delta\beta}$ / $\Delta\beta$)

→ <u>source parameters fully recovered</u> !!!

Summary

Combined EM, particle physics and GW measurements will shed light on binary black hole parameters!

→ a new way to map the Universe!